Cell Reports
Medicine

Article

Safety and immunogenicity of SARS-CoV-2 self-amplifying RNA vaccine expressing an anchored RBD: A randomized, observer-blind phase 1 study

Graphical abstract

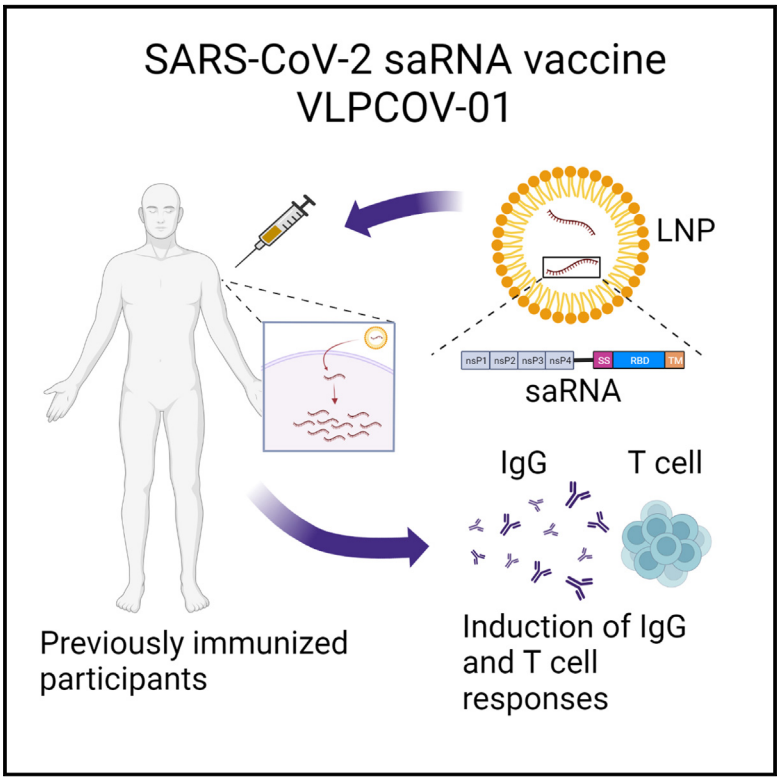

Authors

Wataru Akahata, Takashi Sekida, Takuto Nogimori, ..., Takuya Yamamoto, Jonathan F. Smith, Nobuaki Sato

Correspondence

wakahata@vlptherapeutics.com

In brief

Akahata et al. conduct a phase 1 study in which 96 healthy participants who completed two doses of the BNT162b2 mRNA vaccine are boosted with the SARS-CoV-2 saRNA vaccine VLPCOV-01 or BNT162b2. Equivalent or longer-duration antibody responses are observed with VLPCOV-01 at quantitatively lower RNA doses than BNT162b2.

Highlights

- Booster study of an saRNA SARS-CoV-2 vaccine expressing membrane-anchored RBD
- Robust IgG and T cell responses are induced
- Duration of immunity is equivalent to or longer than that of commercially available vaccines

Akahata et al., 2023, Cell Reports Medicine *4*, 101134
August 15, 2023
https://doi.org/10.1016/j.xcrm.2023.101134

CellPress

Cell Reports Medicine

CellPress
OPEN ACCESS

Article

Safety and immunogenicity of SARS-CoV-2 self-amplifying RNA vaccine expressing an anchored RBD: A randomized, observer-blind phase 1 study

Wataru Akahata,[1,9,*] Takashi Sekida,[1] Takuto Nogimori,[2] Hirotaka Ode,[3] Tomokazu Tamura,[4] Kaoru Kono,[1] Yoko Kazami,[1] Ayaka Washizaki,[2] Yuji Masuta,[2] Rigel Suzuki,[4] Kenta Matsuda,[5] Mai Komori,[5] Amber L. Morey,[5] Keiko Ishimoto,[5] Misako Nakata,[1] Tomoko Hasunuma,[6] Takasuke Fukuhara,[4,7] Yasumasa Iwatani,[3,8] Takuya Yamamoto,[2] Jonathan F. Smith,[5] and Nobuaki Sato[1]

[1]VLP Therapeutics Japan, Inc., Marunouchi, Minato-ku, Tokyo 105-0003, Japan
[2]Laboratory of Precision Immunology, Center for Intractable Diseases and ImmunoGenomics, National Institutes of Biomedical Innovation, Health and Nutrition, Ibaraki, Osaka 567-0085, Japan
[3]Clinical Research Center, National Hospital Organization Nagoya Medical Center, Nagoya, Aichi 460-0001, Japan
[4]Department of Microbiology and Immunology, Faculty of Medicine, Hokkaido University, Sapporo, Hokkaido, Japan
[5]VLP Therapeutics, Inc., Gaithersburg, MD 20878, USA
[6]Department of Research, Kitasato University, Kitasato Institute Hospital, Minato-ku, Tokyo 108-0072, Japan
[7]Laboratory of Virus Control, Research Institute for Microbial Diseases, Osaka University, Suita, Osaka 565-0871, Japan
[8]Division of Basic Medicine, Nagoya University Graduate School of Medicine, Nagoya, Aichi 466-8550, Japan
[9]Lead contact
*Correspondence: wakahata@vlptherapeutics.com
https://doi.org/10.1016/j.xcrm.2023.101134

SUMMARY

VLPCOV-01 is a lipid nanoparticle-encapsulated self-amplifying RNA (saRNA) vaccine that expresses a membrane-anchored receptor-binding domain (RBD) derived from the severe acute respiratory syndrome coronavirus 2 (SARS-CoV-2) spike protein. A phase 1 study of VLPCOV-01 is conducted (jRCT2051210164). Participants who completed two doses of the BNT162b2 mRNA vaccine previously are randomized to receive one intramuscular vaccination of 0.3, 1.0, or 3.0 μg VLPCOV-01, 30 μg BNT162b2, or placebo. No serious adverse events have been reported. VLPCOV-01 induces robust immunoglobulin G (IgG) titers against the RBD protein that are maintained up to 26 weeks in non-elderly participants, with geometric means ranging from 5,037 (95% confidence interval [CI] 1,272–19,940) at 0.3 μg to 12,873 (95% CI 937–17,686) at 3 μg compared with 3,166 (95% CI 1,619–6,191) with 30 μg BNT162b2. Neutralizing antibody titers against all variants of SARS-CoV-2 tested are induced. VLPCOV-01 is immunogenic following low-dose administration. These findings support the potential for saRNA as a vaccine platform.

INTRODUCTION

The coronavirus disease 2019 (COVID-19) pandemic, caused by severe acute respiratory syndrome coronavirus 2 (SARS-CoV-2), has had a significant global impact, with over 699 million cases and more than 6.8 million deaths reported as of March 3, 2023.[1] In response to the emergence of SARS-CoV-2 in Wuhan, China, in December 2019, there was rapid clinical development of SARS-CoV-2 vaccines, with >300 vaccines in development as of May 2022. The World Health Organization (WHO) has approved ten COVID-19 vaccines for global use, reflecting eight distinct vaccine products and four distinct vaccine platforms.[2] Widespread rollout of these vaccines has saved tens of millions of lives.[1,3] Despite the availability of vaccines that have demonstrated efficacy against COVID-19,[4–10] the rapidly changing epidemiology, emergence of new variants, and increased transmissibility despite previous COVID-19 vaccination necessitate new strategies for prevention.[2]

Self-amplifying RNA (saRNA) encapsulated in lipid nanoparticles (LNPs) is a technology for use in vaccines.[11] Vaccines developed using saRNA are promising candidates for meeting the challenges of pandemics because of features including low-dose administration and a readily modifiable antigenic domain, enabling rapid development of vaccines in response to emerging variants of concern.[11,12] We developed an LNP-encapsulated saRNA COVID-19 vaccine (VLPCOV-01) expressing a membrane-anchored receptor-binding domain (RBD) that utilizes an alphavirus RNA amplification system.[13] The self-amplification process results in efficient expression of the gene of interest and a longer duration of expression than those observed with mRNA vaccine platforms.[12] VLPCOV-01 encodes replicase and transcriptase functions composed of the alphavirus non-structural proteins (nsP1–4) from the attenuated TC-83 strain of Venezuelan equine encephalitis virus (VEEV) as well as the RBD of the spike protein from SARS-CoV-2. The RBD sequence is fused with a C-terminal transmembrane domain (RBD-TM), focusing the

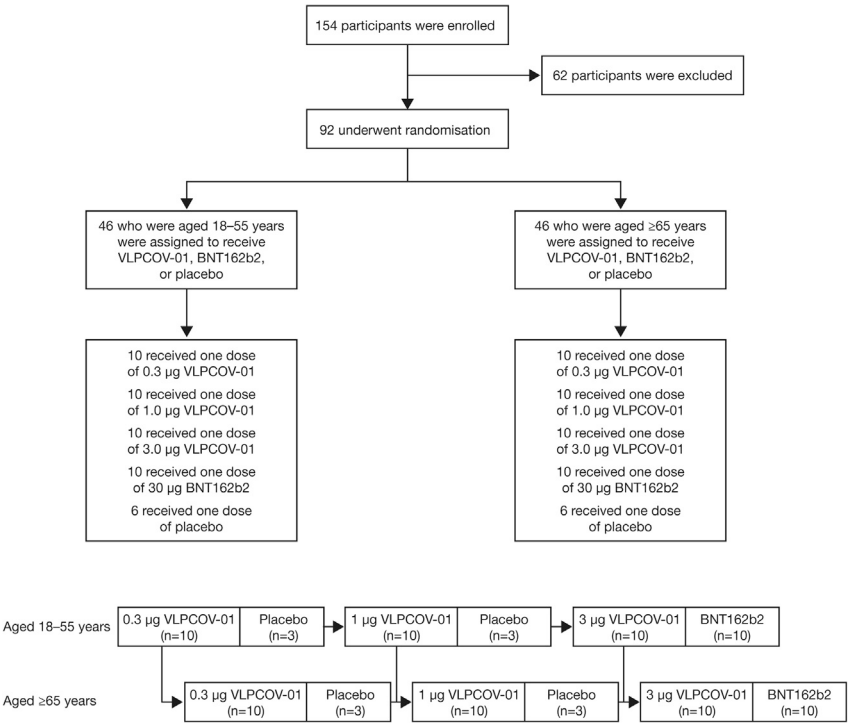

Figure 1. Participant randomization and schedule

The full analysis set and safety analysis set included all participants who underwent randomization and who received one dose of VLPCOV-01, BNT162b2, or placebo. All participants who received injections completed study procedures up to 4 weeks post-study drug administration. For VLPCOV-01 administration, transition from the low-dose cohort to the next dose cohort in the same age group, and from the non-elderly cohort to the elderly cohort, was performed after the principal investigator determined that there were no medical concerns up to day 4.

immune response on the RBD that contains most of the neutralizing epitopes.[14] Preclinical evaluation of VLPCOV-01 in hamster and non-human primate models using LNP delivery systems demonstrated efficient induction of T cell and B cell responses that conferred protection against SARS-CoV-2 challenges. With respect to preclinical challenge studies, non-human primates (NHPs) were immunized twice with saRNA RBD-TM at weeks 0 and 4 and were subsequently challenged with live SARS-CoV-2 Wuhan at week 8. Virus was undetectable in the bronchoalveolar lavage (BAL) at both 2 and 4 days after challenge. Furthermore, RBD-specific antibodies against variants of concern, including Delta and Omicron variants, were maintained for at least 12 months in NHPs.[15]

Here, we present the results of a phase 1 study of VLPCOV-01 in healthy adults who had already received primary vaccination with BNT162b2 to confirm the safety and immunogenicity of VLPCOV-01 as a booster vaccine.

RESULTS

Participants and grouping

A total of 92 participants, 46 in each of the two age groups (non-elderly: 18–55 years old, elderly: over 65 years old) underwent randomization between February 16, 2022 and March 17, 2022. Of the 92 participants who received booster injections, 12 received placebo, 20 received 30 μg BNT162b2, 20 received 3 μg VLPCOV-01, 20 received 1 μg VLPCOV-01, and 20 received 0.3 μg VLPCOV-01. All participants who received injections completed study procedures up to 4 weeks post-study drug administration (Figure 1). The demographic characteristics of the participants at enrollment are shown in Table 1.

Safety profile

No serious adverse events were reported, and no prespecified trial-halting events were met. Following booster vaccination with VLPCOV-01, the majority of solicited adverse events reported were mild to moderate in severity and generally comparable to booster vaccination with BNT162b2 (Figure 2). Among participants in the non-elderly cohort, two participants (20%) who received 3 μg VLPCOV-01 and two participants (20%) who received 30 μg BNT162b2 experienced solicited local adverse events (pain [3 μg VLPCOV-01] and tenderness [30 μg BNT162b2]) that were rated as severe. Two participants (20%) who received 3 μg VLPCOV-01, two participants (20%) who received 1 μg VLPCOV-01, and one participant (10%) who received 30 μg BNT162b2 experienced solicited systemic adverse events (fatigue [3 μg VLPCOV-01], myalgia [3 and 1 μg VLPCOV-01], chills [3 and 1 μg VLPCOV-01 and 30 μg BNT16b2], and arthralgia [3 and 1 μg VLPCOV-01]) that were rated as severe. No solicited adverse events reported by participants aged ≥65 years in the study were classified as severe (Figure 2).

The most common solicited adverse events experienced following VLPCOV-01 vaccination among participants aged 18 to 55 years were pain, tenderness, myalgia, fatigue, headache, chills, and arthralgia and among participants aged ≥65 years were pain, tenderness, and myalgia (Figure 2). Local and systemic reactogenicity events following vaccination with VLPCOV-01 typically occurred on the day of vaccination or one day afterward and were resolved by day 7 (Table S3).

Unsolicited adverse events and clinical laboratory values revealed no patterns of concern and are detailed in Table S4.

Antibody responses

Among non-elderly participants, VLPCOV-01 induced immunoglobulin G (IgG) titers against the SARS-CoV-2 RBD protein (Wuhan variant) that were maintained up to 26 weeks post-vaccination with all doses (Figure 3A). In the non-elderly cohort, IgG titers at 13 weeks post-vaccination in the 3 μg VLPCOV-01 group were 20,833 (95% confidence interval [CI] 8,467–51,261) compared with 6,924.34 (95% CI 3,988–12,021) in the 30 μg BNT162b2 group. IgG titers remained high at 26 weeks post-vaccination

Table 1. Demographic characteristics of the participants at enrollment

	Participants 18–55 years of age					Participants ≥65 years of age				
	VLPCOV-01			BNT162b2	Placebo	VLPCOV-01			BNT162b2	Placebo
	0.3 μg	1.0 μg	3.0 μg	30.0 μg		0.3 μg	1.0 μg	3.0 μg	30.0 μg	
Characteristic	N = 10	N = 10	N = 10	N = 10	N = 6	N = 10	N = 10	N = 10	N = 10	N = 6
Age, years										
Mean ± SD	47.7 ± 6.5	48.8 ± 8.2	44.1 ± 8.2	50.8 ± 3.2	50.8 ± 2.8	71.5 ± 2.9	70.5 ± 3.2	72.0 ± 4.8	68.6 ± 1.8	69.5 ± 3.0
Median (range)	51.0 (36–54)	51.5 (27–54)	48.5 (30–52)	51.0 (45–55)	51.0 (46–54)	71.0 (68–77)	70.5 (65–76)	71.5 (66–78)	69.0 (65–70)	69.0 (66–74)
Gender, n (%)										
Male	3 (30)	0 (0)	5 (50)	3 (30)	2 (33)	8 (80)	4 (40)	5 (50)	4 (40)	3 (50)
Female	7 (70)	10 (100)	5 (50)	7 (70)	4 (67)	2 (20)	6 (60)	5 (50)	6 (60)	3 (50)
Height, cm										
Mean ± SD	162.7 ± 62	156.4 ± 4.6	164.0 ± 9.3	164.2 ± 9.8	159.3 ± 13.0	164.7 ± 8.7	160.2 ± 8.8	160.3 ± 7.7	157.1 ± 5.4	161.3 ± 10.3
Median (range)	162 (156–174)	155 (149–164)	164 (152–181)	163 (150–179)	158 (146–173)	167 (151–178)	159 (148–172)	160 (150–171)	156 (148–164)	162 (144–173)
Weight, kg										
Mean ± SD	60.6 ± 14.7	57.6 ± 11.4	63.6 ± 7.9	65.8 ± 16.5	56.0 ± 13.1	67.4 ± 9.7	57.8 ± 8.9	62.0 ± 7.4	58.0 ± 7.7	64.0 ± 8.8
Median (range)	53.5 (49.4–95.0)	55.2 (46.1–80.5)	63.8 (52.7–77.0)	61.9 (47.3–93.4)	54.5 (43.7–69.7)	68.9 (49.5–82.2)	55.1 (47.2–74.5)	62.1 (49.0–73.9)	60.4 (44.3–70.5)	64.5 (51.9–74.8)
BMI, kg/m^2										
Mean ± SD	22.8 ± 5.2	23.5 ± 4.3	23.7 ± 3.1	24.1 ± 3.6	21.8 ± 1.7	24.8 ± 2.4	22.4 ± 1.8	24.2 ± 3.3	23.4 ± 2.0	24.6 ± 2.7
Median (range)	21.0 (18.6–34.5)	22.4 (19.4–31.8)	22.9 (20.0–30.0)	22.9 (18.2–29.5)	22.0 (20.0–23.3)	24.4 (21.7–30.1)	21.8 (19.4–26.4)	23.0 (19.9–30.0)	23.4 (20.2–26.2)	24.2 (21.8–29.6)
History of allergic reaction, n (%)										
Yes	0 (0)	0 (0)	0 (0)	0 (0)	0 (0)	0 (0)	1 (10)	0 (0)	0 (0)	0 (0)
No	10 (100)	10 (100)	10 (100)	10 (100)	6 (100)	10 (100)	9 (90)	10 (100)	10 (100)	6 (100)
Medical history, n (%)										
Yes	0 (0)	0 (0)	1 (10)	1 (10)	0 (0)	3 (30)	2 (20)	0 (0)	0 (0)	0 (0)
No	10 (100)	10 (100)	9 (90)	9 (90)	6 (100)	7 (70)	8 (80)	10 (100)	10 (100)	6 (100)
Complications, n (%)										
Yes	6 (60)	7 (70)	6 (60	9 (90)	4 (67)	9 (90)	8 (80)	9 (90)	8 (80)	5 (83)
No	4 (40)	3 (30)	4 (40)	1 (10)	2 (33)	1 (10)	2 (20)	1 (10)	2 (20)	1 (17)
Smoker, n (%)										
Yes	1 (10)	1 (10)	2 (20)	0 (0)	2 (33)	0 (0)	1 (10)	2 (20)	2 (20)	0 (0)
No	9 (90)	9 (90)	8 (80)	10 (100)	4 (67)	10 (100)	9 (90)	8 (80)	8 (80)	6 (100)

CellPress
OPEN ACCESS

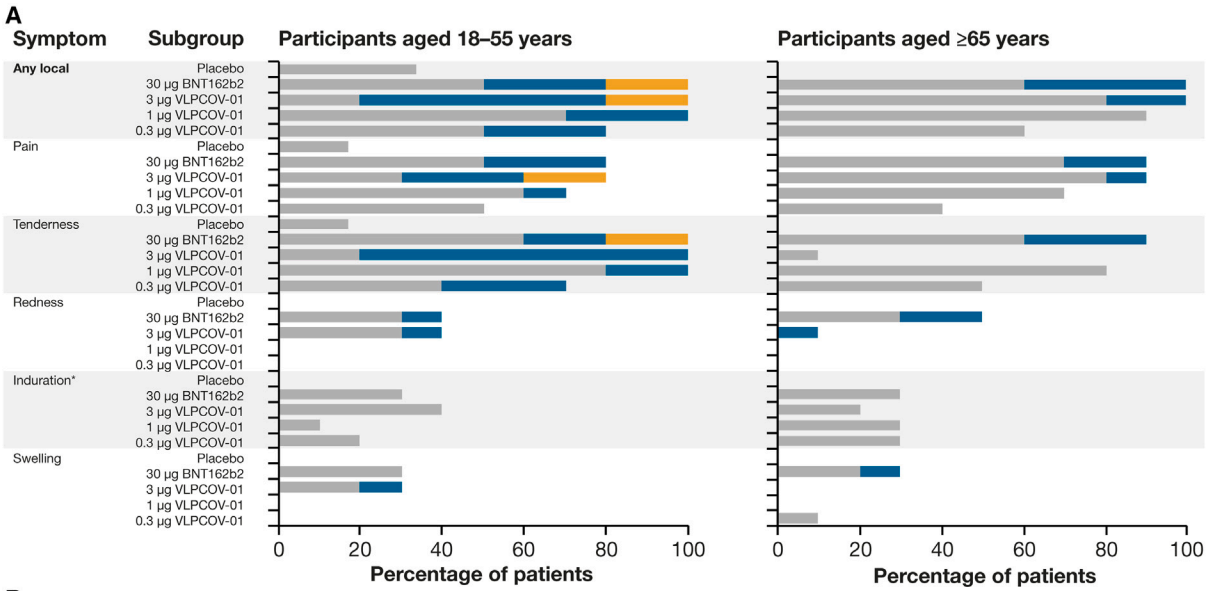

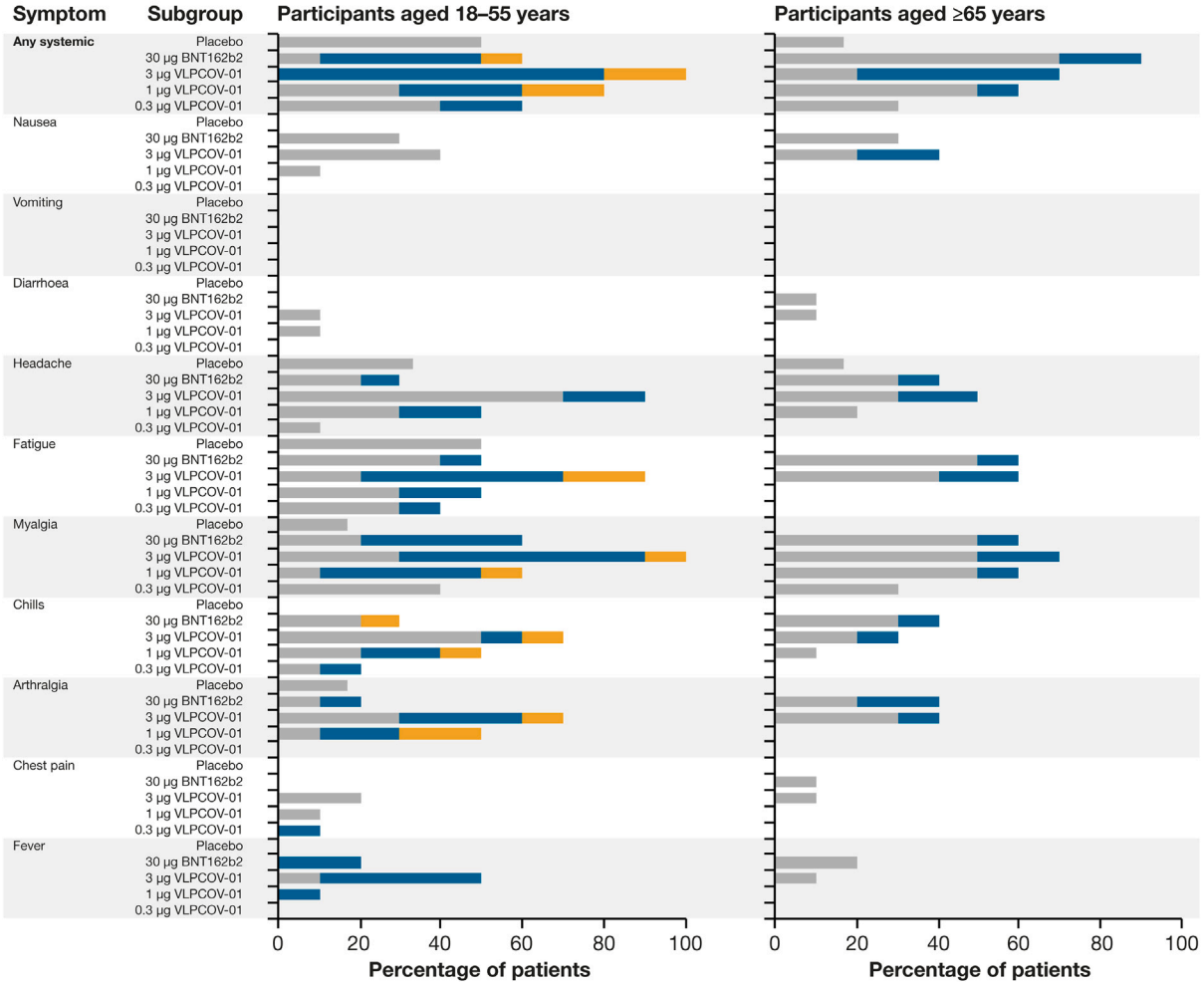

(legend on next page)

with 3 μg VLPCOV-01 and continued to be higher than IgG titers measured following vaccination with 30 μg BNT162b2 (12,873 [95% CI 937–17,686] vs. 3,166 [95% CI 1,619–6,191]). IgG titers at 26 weeks post-vaccination with 1 μg (9,282 [95% CI 2,753–31,299]) and 0.3 μg (5,037 [95% CI 1,272–19,940]) VLPCOV-01 were also higher than IgG titers following vaccination with 30 μg BNT162b2.

In the elderly cohort, all doses of VLPCOV-01 induced IgG titers that were maintained up to 13 weeks post-vaccination. IgG titers at 26 weeks post-vaccination with 3 μg VLPCOV-01 were 9,865 (95% CI 4,396–22,138) compared with 4,183 (95% CI 1,436–12,180) following vaccination with 30 μg BNT162b2.

SARS-CoV-2 neutralization titers were comparable for all groups at baseline. Neutralizing antibody titers against all variants of SARS-CoV-2 tested were induced by all doses of VLPCOV-01 in participants from both age cohorts, and a dose effect was seen (Figure 3B). At 26 weeks post vaccination, results were comparable between 1 and 3 μg VLPCOV-01 and 30 μg BNT162b2. Additionally, inhibition of spike-ACE2 binding and RBD-ACE2 binding for all variants was observed at 26 weeks post vaccination with all concentrations of VLPCOV-01 and in both age cohorts (Figure S1).

A strong correlation was observed between anti-RBD IgG titers and pseudovirus-neutralizing responses to VLPCOV-01 booster vaccination (Figure 3C; $r = 0.950$, $p < 0.001$).

T cell responses

In response to RBD-specific peptide pools, $CD4^+$ T cell responses were induced by booster vaccination with VLPCOV-01 among participants aged 18 to 55 years and ≥65 years (Figures 4A and S2). Across all doses of VLPCOV-01, responses were Th1 dominant (Figure 4B), with minimal Th2 (Figure 4C), Th17 (Figure 4D), and IL-21 (Figure 4E) responses. Responses to spike-specific peptide pools (Figure S3) revealed that, compared with 3 μg VLPCOV-01, 30 μg BNT162b2 induced stronger spike-specific Th1 responses (among non-elderly, geometric mean 1.18- vs. 1.98-fold change; among elderly, geometric mean 1.27- vs. 1.45-fold change), Th2 responses (among non-elderly, geometric mean 1.18- vs. 2.43-fold change; among elderly, geometric mean 1.20- vs. 1.60-fold change), and interleukin-21 (IL-21) responses (among non-elderly, geometric mean 1.49- vs. 8.14-fold change; among elderly, geometric mean 1.70- vs. 4.96-fold change). Exploratory analysis demonstrated a correlation between RBD-specific Th1 responses and neutralizing antibody titers 4 weeks after booster vaccination with VLPCOV-01 (Figure 4F; $r = 0.2717$, $p = 0.0092$). RBD-specific $CD8^+$ T cell responses were also induced by booster vaccination (Figures 4G–4K and S4). The spike-specific $CD8^+$ T cell responses between 30 μg BNT162b2 and 3 μg VLPCOV-01 were at comparable levels (Figure S5). The gating strategies are shown in Figure S6.

Furthermore, analyses of the distribution of IgG subclasses induced by VLPCOV-01 vaccination identified dominant IgG1 responses that were comparable with those induced by BNT162b2 at 4 weeks post-vaccination (Figure S7).

DISCUSSION

Here, we present the findings from the clinical trial of a saRNA vaccine expressing an RBD-anchored antigen. The primary safety and immunogenicity analyses from this phase 1 clinical trial of VLPCOV-01 indicate that in healthy adult participants ≥18 years who have previously received primary COVID-19 vaccination, VLPCOV-01 had an acceptable safety profile and induced high immune responses in both non-elderly and elderly participants, with neutralizing antibody activity strongly correlating with anti-SARS-CoV-2 IgG.

Since the first reported cases of COVID-19 in December 2019, multiple SARS-CoV-2 variants with increased transmissibility and greater antibody escape have emerged.[2] The Omicron variant and its sublineages are highly transmissible, with multiple mutations in the spike protein that result in escape from neutralizing antibody responses that are elicited by COVID-19 vaccination.[16,17] Booster vaccination may lead to an increase in neutralizing antibody titers against Omicron; however, it has been shown that these responses wane after a third dose of mRNA vaccine.[17,18] Mutations in SARS-CoV-2 variants that occur in the spike N-terminal domain or in the RBD, regions that are critical for ACE2 binding, may compromise neutralizing antibody activity.[19] In this study, we demonstrated that VLPCOV-01 booster vaccination elicited broad neutralizing antibody responses, with neutralizing antibody titers to Wuhan (wild type) and the Delta and Omicron variants observed. Furthermore, the neutralizing antibodies were capable of blocking the spike-ACE2 and RBD-ACE2 interactions for all SARS-CoV-2 variants tested.

The COVID-19 mRNA vaccines BNT162b2 and mRNA-1273 have demonstrated waning immunity, with high initial neutralizing antibody titers declining by 3–6 months, necessitating the need for booster vaccinations.[20–22] In this interim analysis, we describe neutralizing activity up to week 26. Further long-term analysis is required to ascertain the duration of response induced by VLPCOV-01; however, the strong correlation of anti-SARS-CoV-2 IgG titers with neutralization suggests that IgG titers may be used as a predictor of neutralizing activity. High IgG titers were maintained up to 13 weeks post-vaccination with VLPCOV-01, and IgG titers measured from samples collected 26 weeks post-vaccination with 3 μg VLPCOV-01 suggest that these may be maintained beyond 6 months. Vogel et al. have monitored the *in vivo* expression of reporter genes (e.g., luciferase) from saRNA vectors, which have shown significantly longer *in vivo* expression than observed with mRNA vectors in mice.[12] The extended expression may contribute to extended duration of immune responses. It is noteworthy that there was a delay in kinetics of antibody response in

Figure 2. Solicited adverse events reported up to 6 days after study drug administration (day 7)

(A) The percentage of solicited local adverse events and their severity reported up to 6 days after study drug administration.

(B) The percentage of systemic adverse events and their severity reported up to 6 days after study drug administration.

The severity of solicited adverse events was graded as mild (gray color), moderate (turquoise color), or severe (orange color) based on criteria that are described in the Table S1. *No severity assessment was made for induration, only a yes or no assessment was made. Percentages shown are participants that recorded "yes."

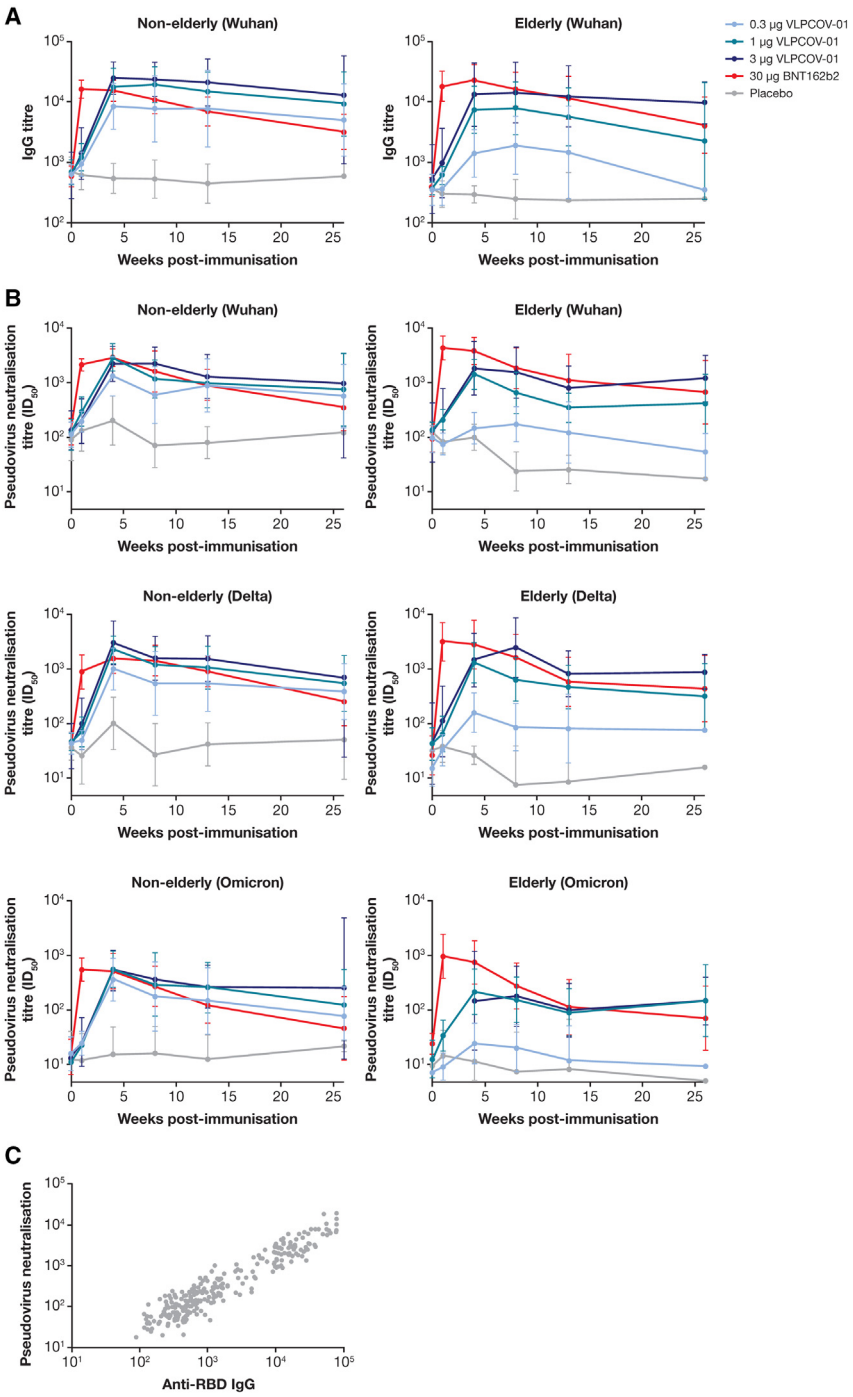

Figure 3. SARS-CoV-2 IgG and neutralizing antibody responses

(A and B) Serum IgG titers against wild-type SARS-CoV-2 RBD protein (A) and pseudovirus neutralizing antibody titers (ID_{50}) against SARS-CoV-2 variants (B) for non-elderly (left side) and elderly (right side) participants (n = 10 per dose group, and n = 6 for the placebo group). Participants received one injection of VLPCOV-01 (0.3, 1.0, or 3.0 μg), 30 μg BNT162b2, or placebo on day 1 (week 0). Logarithmic values are reported as geometric mean titers for serum IgG and neutralizing antibody against pseudovirus. Bars indicate 95% CIs.

(C) The correlation between serum neutralizing antibody titers against pseudovirus Wuhan (wild type) and IgG antibody titers against SARS-CoV-2 RBD protein following booster vaccination.

Pearson's product-moment correlation coefficient and p value were calculated following log transformation of source data ($r = 0.950$, $p < 0.001$).

saRNA groups compared with that of mRNA groups. This may be due to the nature of the saRNA platform, which requires self-amplification to express the antigen. A further investigation of early time points between weeks 1 and 4 is required in future studies. In addition to robust humoral responses, we also demonstrated the ability of VLPCOV-01 to induce RBD-specific $CD4^+$ and $CD8^+$ T cell responses that were comparable to BNT162b2. Although whole spike-specific $CD4^+$ T cell responses were higher in BNT162b2 compared to VLPCOV-01 (Figure S4), the correlation between RBD-specific Th1 responses and neutralizing antibody titers 4 weeks following booster vaccination with VLPCOV-01 (Figure 4) suggests that $CD4^+$ T cell induction is sufficient to help maintain neutralizing activity. Moreover, total RBD-specific $CD4^+$ T cells ($CD154^+$) were dominated by Th1 cells, which is consistent with the reported T cell responses for other COVID-19 vaccines.[23–27]

Studies have demonstrated the importance of vaccine-elicited T cell responses in coordinating humoral and cellular immune responses and their extended durability despite declining antibody titers.[28,29] The VLPCOV-01-induced T cell responses that formed across both age cohorts may therefore provide critical protection from severe illness due to SARS-CoV-2 infection.

Limitations of this study include the relatively short follow up to date and small trial size, particularly at later immunogenicity analysis time points, where the number of participants in the analysis decreased over time because of vaccination with authorized vaccines post-week 4 or because of infection with SARS-CoV-2. The number of participants that received authorized vaccine in the elderly group was higher than that in the non-elderly group. There are several potential explanations for this bias. The proportion of vaccinated individuals in the elderly population is over 85% in Japan, indicating that they are more likely to receive a booster vaccine. There is also a psychological factor that may have played a role in this bias. The informed consent indicates that low-dose groups include placebo, which may have encouraged them to take a publicly available vaccine. Adverse event reporting is

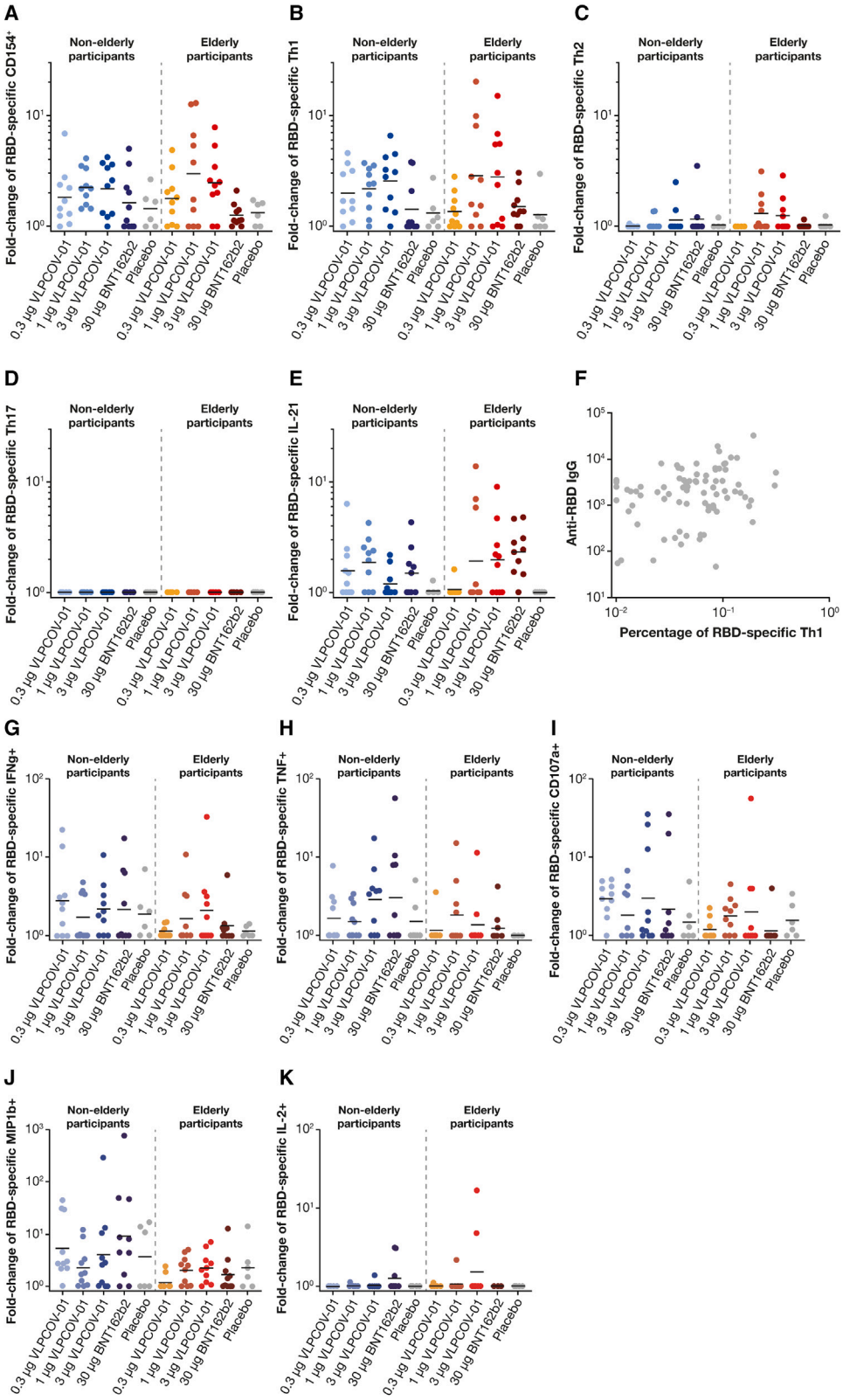

(legend on next page)

ongoing and will continue until the planned study duration of 52 weeks. We are conducting a phase 2 dose-ranging study to further evaluate the immunogenicity response and safety profile of VLPCOV-01. Reactogenicity of VLPCOV-01 appears to be similar to that of BNT162b2 regardless of 10-fold difference in dose. The saRNA platform is more prone to degradation or premature termination of transcripts during the production of RNA due to its size. Exclusion of this degraded or premature RNA during production may not only reduce the reactogenicity but could improve the immunogenicity per dose. These factors may have contributed to the level of reactogenicity of VLPCOV-01, which we are planning to address in the upcoming clinical trial.

There are other COVID-19 vaccines in clinical development that either utilize the saRNA vaccine platform[11] or specifically target the RBD of the spike protein.[30] However, to our knowledge, this is the first report from a clinical study of a COVID-19 vaccine that encompasses both the saRNA platform and RBD-anchored antigen design. We have shown that VLPCOV-01 has a favorable safety profile and induces immune responses that are comparable to the BNT162b2 mRNA vaccine. Importantly, the responses induced by VLPCOV-01 are achieved at 1/10 of the BNT162b2 dose with potentially longer duration, which is advantageous when considering the importance of being able to produce vaccines in large quantities to meet the demands of the COVID-19 pandemic. A low-dose vaccine such as VLPCOV-01 enables production of more doses for the same amount of vaccine, improving manufacturing scale and time and increasing distribution volume. Overall, the results from this study suggest that VLPCOV-01 could be used as an alternative to the mRNA vaccines that are currently available for COVID-19 booster vaccination and support further development of this vaccine.

Limitations of the study

This study has some limitations. The small sample size restricted the interpretation of a definite conclusion, especially at later time points, because of a reduction in the sample size over time. Further research on the immunogenicity and efficacy of VLPCOV-01 with increased sample size is necessary.

STAR★METHODS

Detailed methods are provided in the online version of this paper and include the following:

SUPPLEMENTAL INFORMATION

Supplemental information can be found online at https://doi.org/10.1016/j.xcrm.2023.101134.

ACKNOWLEDGMENTS

This study was supported by AMED, Japan under grant number JP21nf0101627. Medical writing support was provided by Emily Feist, PhD, of Parexel International, which was funded by VLP Therapeutics Japan, Inc. VLP Therapeutics Japan, Inc. served as the trial sponsor and was responsible for the design and conduct of the trial, for the collection, analysis, and interpretation of the data, and for the writing of the manuscript. AMED, who provided funding for the study, had no role in study design, data collection, data analysis, data interpretation, or writing of the report.

AUTHOR CONTRIBUTIONS

T.S., N.S., Y.I., T.F., T.Y., J.F.S., and W.A. conceived, designed, and coordinated the study. T.N., A.W., and Y.M. performed T cell analysis. H.O., T.T., and R.S. performed IgG analysis. Y.K., N.S., K.K., T.S., M.N., and T.H. prepared and executed the clinical study. M.K., T.N., K.I., A.M., T.Y., K.M., and W.A. contributed to the data validation, analysis, and writing and revision of the manuscript. All authors read and approved the manuscript, had full access to all the data in the study, and had final responsibility for the decision to submit for publication.

Figure 4. $CD4^+$ T cell responses

Flow cytometric analysis was performed to analyze RBD-specific T cells. Responses to VLPCOV-01, BNT162b2, or placebo are shown as fold change from baseline (day 1) to week 4 (day 29) for each cohort. The experiment was performed once.

(A) The activated $CD4^+$ T cells, characterized by the expression of CD154.

(B) The response in $CD4^+$ Th1 cells was characterized by the expression of interleukin-2, tumor necrosis factor α, and/or interferon-γ.

(C) The response in $CD4^+$ Th2 cells, which was measured by expression of interleukin-4 and/or -13.

(D) The response in $CD4^+$ Th17 cells, characterized by the expression of interleukin-17.

(E) The $CD4^+$ IL-21+ cells, which were measured by expression of IL-21.

(F) The correlation between IgG antibody titers against SARS-CoV-2 RBD protein and the percentage of RBD-specific $CD4^+$ Th1 cell responses following vaccination with VLPCOV-01. Spearman's rank correlation coefficient and p value were calculated following log transformation of source data ($r = 0.2717$, $p = 0.0092$).

(G–K) $CD8^+$ cells expressing interferon-γ, tumor necrosis factor α, CD107a, macrophage inflammatory protein 1b, or interleukin-2, respectively.

(A–E and G–K) The horizontal bars indicate geometric mean value.

DECLARATION OF INTERESTS

M.K., A.M., K.I., and K.M. are employees of VLP Therapeutics, Inc.; W.A. is a board member of, an employee of, and holds stocks in VLP Therapeutics, Inc. and is a management board member of VLP Therapeutics Japan, Inc.; J.F.S. and M.N. are employees of and hold stocks in VLP Therapeutics, Inc.; T.S., N.S., K.K., and Y.K. are employees of VLP Therapeutics Japan, Inc.; T.H. received a consultation fee from VLP Therapeutics Japan, Inc. for medical advice and consultation on clinical trial design; and W.A. and J.F.S. are inventors on a related vaccine patent.

INCLUSION AND DIVERSITY

We support inclusive, diverse, and equitable conduct of research.

Received: November 28, 2022
Revised: March 16, 2023
Accepted: July 7, 2023
Published: August 15, 2023

REFERENCES

1. World Health Organization. WHO Coronavirus (COVID-19) dashboard. https://COVID19.who.int/(accessed November 08.
2. Barouch, D.H. (2022). Covid-19 Vaccines - Immunity, Variants, Boosters. N. Engl. J. Med. *387*, 1011–1020. https://doi.org/10.1056/NEJMra2206573.
3. Watson, O.J., Barnsley, G., Toor, J., Hogan, A.B., Winskill, P., and Ghani, A.C. (2022). Global impact of the first year of COVID-19 vaccination: a mathematical modelling study. Lancet Infect. Dis. *22*, 1293–1302. https://doi.org/10.1016/S1473-3099(22)00320-6.
4. Baden, L.R., El Sahly, H.M., Essink, B., Kotloff, K., Frey, S., Novak, R., Diemert, D., Spector, S.A., Rouphael, N., Creech, C.B., et al. (2021). Efficacy and Safety of the mRNA-1273 SARS-CoV-2 Vaccine. N. Engl. J. Med. *384*, 403–416. https://doi.org/10.1056/NEJMoa2035389.
5. Ella, R., Reddy, S., Blackwelder, W., Potdar, V., Yadav, P., Sarangi, V., Aileni, V.K., Kanungo, S., Rai, S., Reddy, P., et al. (2021). Efficacy, safety, and lot-to-lot immunogenicity of an inactivated SARS-CoV-2 vaccine (BBV152): interim results of a randomised, double-blind, controlled, phase 3 trial. Lancet *398*, 2173–2184. https://doi.org/10.1016/S0140-6736(21)02000-6.
6. Falsey, A.R., Sobieszczyk, M.E., Hirsch, I., Sproule, S., Robb, M.L., Corey, L., Neuzil, K.M., Hahn, W., Hunt, J., Mulligan, M.J., et al. (2021). Phase 3 Safety and Efficacy of AZD1222 (ChAdOx1 nCoV-19) Covid-19 Vaccine. N. Engl. J. Med. *385*, 2348–2360. https://doi.org/10.1056/NEJMoa2105290.
7. Heath, P.T., Galiza, E.P., Baxter, D.N., Boffito, M., Browne, D., Burns, F., Chadwick, D.R., Clark, R., Cosgrove, C., Galloway, J., et al. (2021). Safety and Efficacy of NVX-CoV2373 Covid-19 Vaccine. N. Engl. J. Med. *385*, 1172–1183. https://doi.org/10.1056/NEJMoa2107659.
8. Polack, F.P., Thomas, S.J., Kitchin, N., Absalon, J., Gurtman, A., Lockhart, S., Perez, J.L., Pérez Marc, G., Moreira, E.D., Zerbini, C., et al. (2020). Safety and Efficacy of the BNT162b2 mRNA Covid-19 Vaccine. N. Engl. J. Med. *383*, 2603–2615. https://doi.org/10.1056/NEJMoa2034577.
9. Sadoff, J., Gray, G., Vandebosch, A., Cárdenas, V., Shukarev, G., Grinsztejn, B., Goepfert, P.A., Truyers, C., Fennema, H., Spiessens, B., et al. (2021). Safety and Efficacy of Single-Dose Ad26.COV2.S Vaccine against Covid-19. N. Engl. J. Med. *384*, 2187–2201. https://doi.org/10.1056/NEJMoa2101544.
10. Tanriover, M.D., Doğanay, H.L., Akova, M., Güner, H.R., Azap, A., Akhan, S., Köse, Ş., Erdinç, F.Ş., Akalın, E.H., Tabak, Ö.F., et al. (2021). Efficacy and safety of an inactivated whole-virion SARS-CoV-2 vaccine (CoronaVac): interim results of a double-blind, randomised, placebo-controlled, phase 3 trial in Turkey. Lancet *398*, 213–222. https://doi.org/10.1016/S0140-6736(21)01429-X.
11. Pollock, K.M., Cheeseman, H.M., Szubert, A.J., Libri, V., Boffito, M., Owen, D., Bern, H., O'Hara, J., McFarlane, L.R., Lemm, N.M., et al. (2022). Safety and immunogenicity of a self-amplifying RNA vaccine against COVID-19: COVAC1, a phase I, dose-ranging trial. EClinicalMedicine *44*, 101262. https://doi.org/10.1016/j.eclinm.2021.101262.
12. Vogel, A.B., Lambert, L., Kinnear, E., Busse, D., Erbar, S., Reuter, K.C., Wicke, L., Perkovic, M., Beissert, T., Haas, H., et al. (2018). Self-Amplifying RNA Vaccines Give Equivalent Protection against Influenza to mRNA Vaccines but at Much Lower Doses. Mol. Ther. *26*, 446–455. https://doi.org/10.1016/j.ymthe.2017.11.017.
13. Pushko, P., Parker, M., Ludwig, G.V., Davis, N.L., Johnston, R.E., and Smith, J.F. (1997). Replicon-helper systems from attenuated Venezuelan equine encephalitis virus: expression of heterologous genes in vitro and immunization against heterologous pathogens in vivo. Virology *239*, 389–401. https://doi.org/10.1006/viro.1997.8878.
14. Piccoli, L., Park, Y.J., Tortorici, M.A., Czudnochowski, N., Walls, A.C., Beltramello, M., Silacci-Fregni, C., Pinto, D., Rosen, L.E., Bowen, J.E., et al. (2020). Mapping Neutralizing and Immunodominant Sites on the SARS-CoV-2 Spike Receptor-Binding Domain by Structure-Guided High-Resolution Serology. Cell *183*, 1024–1042.e21. https://doi.org/10.1016/j.cell.2020.09.037.
15. Komori, M., Nogimori, T., Morey, A.L., Sekida, T., Ishimoto, K., Hassett, M.R., Masuta, Y., Ode, H., Tamura, T., Suzuki, R., et al. (2023). saRNA vaccine expressing membrane-anchored RBD elicits broad and durable immunity against SARS-CoV-2 variants of concern. Nat Commun *14*, 2810. https://doi.org/10.1038/s41467-023-38457-x.
16. Iketani, S., Liu, L., Guo, Y., Liu, L., Chan, J.F.W., Huang, Y., Wang, M., Luo, Y., Yu, J., Chu, H., et al. (2022). Antibody evasion properties of SARS-CoV-2 Omicron sublineages. Nature *604*, 553–556. https://doi.org/10.1038/s41586-022-04594-4.
17. Liu, L., Iketani, S., Guo, Y., Chan, J.F.W., Wang, M., Liu, L., Luo, Y., Chu, H., Huang, Y., Nair, M.S., et al. (2022). Striking antibody evasion manifested by the Omicron variant of SARS-CoV-2. Nature *602*, 676–681. https://doi.org/10.1038/s41586-021-04388-0.
18. Pajon, R., Doria-Rose, N.A., Shen, X., Schmidt, S.D., O'Dell, S., McDanal, C., Feng, W., Tong, J., Eaton, A., Maglinao, M., et al. (2022). SARS-CoV-2 Omicron Variant Neutralization after mRNA-1273 Booster Vaccination. N. Engl. J. Med. *386*, 1088–1091. https://doi.org/10.1056/NEJMc2119912.
19. Zhang, S., Gao, C., Das, T., Luo, S., Tang, H., Yao, X., Cho, C.Y., Lv, J., Maravillas, K., Jones, V., et al. (2022). The spike-ACE2 binding assay: An in vitro platform for evaluating vaccination efficacy and for screening SARS-CoV-2 inhibitors and neutralizing antibodies. J. Immunol. Methods *503*, 113244. https://doi.org/10.1016/j.jim.2022.113244.
20. Collier, A.R.Y., Yu, J., McMahan, K., Liu, J., Chandrashekar, A., Maron, J.S., Atyeo, C., Martinez, D.R., Ansel, J.L., Aguayo, R., et al. (2021). Differential Kinetics of Immune Responses Elicited by Covid-19 Vaccines. N. Engl. J. Med. *385*, 2010–2012. https://doi.org/10.1056/NEJMc2115596.
21. Falsey, A.R., Frenck, R.W., Jr., Walsh, E.E., Kitchin, N., Absalon, J., Gurtman, A., Lockhart, S., Bailey, R., Swanson, K.A., Xu, X., et al. (2021). SARS-CoV-2 Neutralization with BNT162b2 Vaccine Dose 3. N. Engl. J. Med. *385*, 1627–1629. https://doi.org/10.1056/NEJMc2113468.
22. Pegu, A., O'Connell, S.E., Schmidt, S.D., O'Dell, S., Talana, C.A., Lai, L., Albert, J., Anderson, E., Bennett, H., Corbett, K.S., et al. (2021). Durability of mRNA-1273 vaccine-induced antibodies against SARS-CoV-2 variants. Science *373*, 1372–1377. https://doi.org/10.1126/science.abj4176.
23. Anderson, E.J., Rouphael, N.G., Widge, A.T., Jackson, L.A., Roberts, P.C., Makhene, M., Chappell, J.D., Denison, M.R., Stevens, L.J., Pruijssers, A.J., et al. (2020). Safety and Immunogenicity of SARS-CoV-2 mRNA-1273 Vaccine in Older Adults. N. Engl. J. Med. *383*, 2427–2438. https://doi.org/10.1056/NEJMoa2028436.
24. Jackson, L.A., Anderson, E.J., Rouphael, N.G., Roberts, P.C., Makhene, M., Coler, R.N., McCullough, M.P., Chappell, J.D., Denison, M.R., Stevens, L.J., et al. (2020). An mRNA Vaccine against SARS-CoV-2 - Preliminary Report. N. Engl. J. Med. *383*, 1920–1931. https://doi.org/10.1056/NEJMoa2022483.

25. Keech, C., Albert, G., Cho, I., Robertson, A., Reed, P., Neal, S., Plested, J.S., Zhu, M., Cloney-Clark, S., Zhou, H., et al. (2020). Phase 1-2 Trial of a SARS-CoV-2 Recombinant Spike Protein Nanoparticle Vaccine. N. Engl. J. Med. *383*, 2320–2332. https://doi.org/10.1056/NEJMoa2026920.

26. Sadoff, J., Le Gars, M., Shukarev, G., Heerwegh, D., Truyers, C., de Groot, A.M., Stoop, J., Tete, S., Van Damme, W., Leroux-Roels, I., et al. (2021). Interim Results of a Phase 1-2a Trial of Ad26.COV2.S Covid-19 Vaccine. N. Engl. J. Med. *384*, 1824–1835. https://doi.org/10.1056/NEJMoa2034201.

27. Sahin, U., Muik, A., Derhovanessian, E., Vogler, I., Kranz, L.M., Vormehr, M., Baum, A., Pascal, K., Quandt, J., Maurus, D., et al. (2020). COVID-19 vaccine BNT162b1 elicits human antibody and T(H)1 T cell responses. Nature *586*, 594–599. https://doi.org/10.1038/s41586-020-2814-7.

28. Goel, R.R., Painter, M.M., Apostolidis, S.A., Mathew, D., Meng, W., Rosenfeld, A.M., Lundgreen, K.A., Reynaldi, A., Khoury, D.S., Pattekar, A., et al. (2021). mRNA vaccines induce durable immune memory to SARS-CoV-2 and variants of concern. Science *374*, abm0829. https://doi.org/10.1126/science.abm0829.

29. Painter, M.M., Mathew, D., Goel, R.R., Apostolidis, S.A., Pattekar, A., Kuthuru, O., Baxter, A.E., Herati, R.S., Oldridge, D.A., Gouma, S., et al. (2021). Rapid induction of antigen-specific CD4(+) T cells is associated with coordinated humoral and cellular immunity to SARS-CoV-2 mRNA vaccination. Immunity *54*, 2133–2142.e3. https://doi.org/10.1016/j.immuni.2021.08.001.

30. Thuluva, S., Paradkar, V., Gunneri, S.R., Yerroju, V., Mogulla, R., Turaga, K., Kyasani, M., Manoharan, S.K., Medigeshi, G., Singh, J., et al. (2022). Evaluation of safety and immunogenicity of receptor-binding domain-based COVID-19 vaccine (Corbevax) to select the optimum formulation in open-label, multicentre, and randomised phase-1/2 and phase-2 clinical trials. EBioMedicine *83*, 104217. https://doi.org/10.1016/j.ebiom.2022.104217.

31. Matsuura, Y., Tani, H., Suzuki, K., Kimura-Someya, T., Suzuki, R., Aizaki, H., Ishii, K., Moriishi, K., Robison, C.S., Whitt, M.A., and Miyamura, T. (2001). Characterization of pseudotype VSV possessing HCV envelope proteins. Virology *286*, 263–275. https://doi.org/10.1006/viro.2001.0971.

32. Nogimori, T., Moriishi, E., Ikeda, M., Takahama, S., and Yamamoto, T. (2021). OMIP 075: A 22-color panel for the measurement of antigen-specific T-cell responses in human and nonhuman primates. Cytometry A. *99*, 884–887. https://doi.org/10.1002/cyto.a.24460.

33. Tani, H., Komoda, Y., Matsuo, E., Suzuki, K., Hamamoto, I., Yamashita, T., Moriishi, K., Fujiyama, K., Kanto, T., Hayashi, N., et al. (2007). Replication-competent recombinant vesicular stomatitis virus encoding hepatitis C virus envelope proteins. J. Virol. *81*, 8601–8612. https://doi.org/10.1128/JVI.00608-07.

STAR★METHODS

KEY RESOURCES TABLE

REAGENT or RESOURCE	SOURCE	IDENTIFIER
Antibodies		
Mouse anti-human CD154-FITC (clone: TRAP1)	BD Biosciences	cat# 555699; RRID: AB_396049
Mouse anti-human CD3-BUV615 (clone: SP34-2)	BD Biosciences	cat# 751249; RRID: AB_2875266
Mouse anti-human CD4-PE-Cy5.5 (clone: S3.5)	Thermo Ficher Scientific	cat# MHCD0418; RRID: AB_10376013
Mouse anti-human CD8-BUV563 (clone: RPA-T8)	BD Biosciences	cat# 612914; RRID: AB_2870200
Mouse anti-human CD27-PE-Cy5 (clone: 1A4CD27)	Beckman coulter	cat# 6607107
Mouse anti-human CD45RO-BUV805 (clone: UCHL1)	BD Biosciences	cat# 748367; RRID: AB_2872786
Mouse anti-human IFN-g-BV786 (clone: 4S.B3)	BioLegend	cat# 502542; RRID: AB_2563882
Mouse anti-human TNF-BV650 (clone: MAb11)	BioLegend	cat# 502938; RRID: AB_2562741
Rat anti-human IL-13-BV421 (clone: JES10-5A2)	BD Biosciences	cat# 563580; RRID: AB_2738290
Mouse anti-human IL-21-Ax647 (clone: 3A3-N21)	BD Biosciences	cat# 560493; RRID: AB_1645421
Mouse anti-human IL-4-PE-Cy7 (clone:8D4-8)	BD Biosciences	cat# 560672; RRID: AB_1727547
Mouse anti-human IL-17A-BV605 (clone: BL168)	BioLegend	cat# 512326; RRID: AB_2563887
Rat anti-human IL-2-BUV737 (clone: MQ1-17H12)	BD Biosciences	cat# 612836
Mouse anti-human CD107A-BV711 (clone: H4A3)	BioLegend	cat# 328640; RRID: AB_2565840
Mouse anti-human MIP1b-Alexa700 (clone: D21-1351)	BD Biosciences	cat# 561278; RRID: AB_10612008
Anti-SARS-CoV-2 Spike RBD Neutralizing Antibody, Human IgG1 (AS35)	ACROBiosystems	cat# SAD-S35
Anti-SARS-CoV-2 Spike RBD Neutralizing Antibody, Human IgG2 (AS35)	ACROBiosystems	cat# SAD-S66
Anti-SARS-CoV-2 Spike RBD Neutralizing Antibody, Human IgG3 (AS35)	ACROBiosystems	cat# SAD-S67
Anti-SARS-CoV-2 Spike RBD Neutralizing Antibody, Human IgG4 (AS35)	ACROBiosystems	cat# SAD-S68
Mouse anti-Human IgG1 Fc Secondary Antibody, HRP	Thermo Fisher Scientific	cat# MH1715; RRID: AB_2539710
Mouse Anti-Human IgG2 Fc-BIOT HP6002	SouthernBiotech	cat# 9070-08; RRID: AB_2796638
Mouse Anti-Human IgG3 Hinge-BIOT HP6050	SouthernBiotech	cat# 9210-08; RRID: AB_2796700
Mouse Anti-Human IgG4 Fc-BIOT HP6025	SouthernBiotech	cat# 9200-08; RRID: AB_2796692
Biological samples		
Human PBMCs	This study	This study
Chemicals, peptides, and recombinant proteins		
Benzonase Nuclease, Purity >90%	MERCK Millipore	cat# 70746

(*Continued on next page*)

Continued

REAGENT or RESOURCE	SOURCE	IDENTIFIER
BD GolgiPlug	BD Biosciences	cat# 555029
BD GolgiStop	BD Biosciences	cat# 554724
LIVE/DEADTM Fixable Blue Dead Cell Stain Kit	Thermo Fisher Scientific	cat# L23105
Cytofix/Cytoperm kit	BD Biosciences	cat# 554714
RBD protein	SinoBiological	cat# 40592-VNAH
Peroxidase Substrate Solution B	KPL	cat# 50-65-02
TMB Peroxidase Substrate	KPL	cat# 50-76-02
HRP-conjugated streptavidin	Thermo Fisher Scientific	cat# N100
Peptide sequence for T cell analysis (See Table S5)	This paper	N/A
TransIT-LT1	Mirus Bio	MIR2300
pCAGG -SARS-CoV-2-Wuhan spike	This paper	N/A
pCAGG -SARS-CoV-2- Delta spike	This paper	N/A
pCAGG -SARS-CoV-2- Omicron BA.2 spike	This paper	N/A
VSVΔG-Luc/G	Matsuura et al.[31]	N/A
VSVΔG-Luc/SARS-CoV-2 Wuhan spike	This paper	N/A
VSVΔG-Luc/SARS-CoV-2 Delta spike	This paper	N/A
VSVΔG-Luc/SARS-CoV-2 Omicron BA.2 spike	This paper	N/A
Luciferase assay system	Promega	E1500
Critical commercial assays		
V-PLEX SARS-CoV-2 Panel 7 (ACE2) multiplexed immunoassay kit	Meso Scale Diagnostics	Cat# K15440U-2 and K15440U-4
Deposited data		
SARS-COV-2 Wuhan signal sequence	GenBank	YP_009724390.1 amino acids [aa] 1–13 of S
SARS-COV-2 Wuhan RBD sequence	GenBank	YP_009724390.1 amino acids [aa] 327–531 of S
Influenza hemagglutinin (HA) sequence	GenBank	P03452.2 [aa] 518-565
SARS-CoV-2 Wuhan spike gene	GenBank	NC_045512.2
SARS-CoV-2 Delta spike gene	GenBank	QWA53965.1
SARS-CoV-2 Omicron spike gene	GenBank	UFO69279.1
Experimental models: Cell lines		
HEK239T cells	ATCC	CRL-3216
Vero cells	ATCC	CCL-81
Software and algorithms		
Discovery Workbench software 4.0	Meso Scale Diagnostics	https://www.mesoscale.com/en/products_and_services/software
FlowJo 10.7.1	BD Biosciences	https://www.flowjo.com/
GraphPadPrism version 8	GraphPad Software, Inc.	https://www.graphpad.com
GraphPadPrism version 9	GraphPad Software, Inc.	https://www.graphpad.com

RESOURCE AVAILABILITY

Lead contact

Further information and requests for resources and reagents should be directed to and will be fulfilled by the lead contact, Wataru Akahata (wakahata@vlptherapeutics.com).

Materials availability

This study did not generate new unique reagents.

Data and code availability

- The published article includes all data generated or analyzed during this study, which is summarized in the accompanying tables, figures, and supplemental materials.
- The code to T cell peptide epitopes has been deposited in the Mendeley, is publicly available as of the date of publication, and can be accessed with the following link: https://doi.org/10.17632/k7zf8893x2.1.
- Any additional information required to reanalyze the data reported in this paper is available from the lead contact upon request.
- Access to related study documents (e.g., study protocol, statistical analysis plan, clinical study report) will be provided upon request from qualified researchers, and is subject to certain criteria, conditions, and exceptions.

EXPERIMENTAL MODEL AND STUDY PARTICIPANT DETAILS

Study participant details

Ninety-two healthy Japanese adults (55 female and 37 male) aged 18 to 55 or ≥65 years who had completed two doses of the mRNA vaccine BNT162b2 6 to 12 months previously were recruited. Demographic information along with the key inclusion criteria and exclusion criteria were provided. The study protocol was reviewed and approved by the Medical Corporation Heishinkai OPHAC Hospital institutional review board, and the trial was conducted at Medical Corporation Heishinkai OPHAC Hospital. No important changes to the methods were made following trial commencement.

Cell lines

HEK293T cells (Female, human embryonic kidney cells) were maintained in DMEM supplemented with 10% FBS and 2mM L-glutamine at 37°C. The Vero cells (kidney epithelial cells extracted from an African green monkey) are maintained in DMEM supplemented with 10% FBS at 37°C. Peripheral blood mononuclear cells (PBMCs) obtained from participants were maintained in RPMI medium containing 10% FBS at 37°C.

METHOD DETAILS

Antigen design and LNPs

The antigen expressed from the saRNA vector was constructed as a membrane-anchored RBD (RBD-TM) using the SARS-CoV-2 signal sequence (Wuhan GenBank# YP_009724390.1 amino acids [aa] 1–13 of S) fused to the Wuhan RBD sequence (aa 327–531 of S) with an influenza hemagglutinin (HA) transmembrane and cytoplasmic tail domain (aa positions 518–565, GenBank#P03452.2). The saRNA was encapsulated in LNPs using a microfluidics method in which an aqueous solution of saRNA at pH = 4.0 was rapidly mixed with an ethanol solution of lipids from the FUJIFILM Corporation. LNPs used in this study contained a propriety mixture of ionizable lipid. phospholipid, cholesterol, and PEG-lipid. The proprietary lipids and LNPs are prepared with reference to the patent (WO2021/095876).

Study design and participants

We assessed the safety, immunogenicity, and dosage of a single booster dose of VLPCOV-01 in a randomised, single-centre, placebo- and active-controlled, observer-blind phase 1 study.

The planned number of participants as set out in the study protocol was 92. This was deemed an appropriate target to evaluate the immunogenicity and safety of the investigational drug. Eligible participants were healthy Japanese adults aged 18 to 55 or ≥65 years who had completed two doses of the mRNA vaccine BNT162b2 6 to 12 months previously. Key exclusion criteria were a history of COVID-19, pregnant and lactating females, a history or presence of a serious cardiovascular, haematological, respiratory, hepatic, renal, gastrointestinal, and/or neuropsychiatric disease, and previously received or planned to receive treatment with any drug or therapy considered to affect the immunogenicity assessments. The criteria for discontinuation/dropout from the study for an individual subjects were safety issues, unable to comply with the protocol, and when subject was found to be unsuitable for inclusion criteria for the study. All participants provided written informed consent before enrollment. Full eligibility criteria are described in the study protocol.

Randomization and masking

The principal investigator appointed a study drug randomization supervisor who prepared the randomization schedule prior to participant enrollment and was responsible for storing and managing it until study unblinding. Potential participants were assigned a screening number by the principal or sub investigator, assessed for suitability to participate in the study, and upon completion of screening, were allocated a participant identification code. Participants were stratified into two age subgroups: 18 to 55 years (non-elderly cohort) and ≥65 years (elderly cohort). Participants in each group were randomised to receive VLPCOV-01 at doses

of 0 · 3, 1 · 0, or 3 · 0 μg, 30-μg BNT162b2, or placebo. Transition to the next VLPCOV-01 dose cohort in the same age group, and from the non-elderly cohort to the elderly cohort, was performed after the principal investigator determined that there were no medical concerns based on the results of the tests and examinations performed up to day 4 for each cohort. Assessors and participants were blinded for the study. The principal investigator assigned unblinded medical staff in advance who allocated, prepared and administered the study drugs and were not involved in the assessments of participants after administration.

Procedures

The investigational vaccine, VLPCOV-01, was compared to 30 μg BNT162b2 and placebo (0 · 9% saline). VLPCOV-01, developed by VLP Therapeutics, is a saRNA vaccine against COVID-19, stabilised by and delivered with LNPs. The saRNA expresses the nonstructural proteins of the alphavirus from the 5′ end of the RNA, as well as an engineered RBD sequence of SARS-CoV-2 (Wuhan stain; GenBank Yp_009724390.1) from the subgenomic promoter, thus allowing amplification of the replicon RNA in transfected cells and high-level expression of the RBD construct. All study drugs were stored in accordance with study drug management procedures.

The study drug was administered as a single dose by the intramuscular route into the deltoid region of the upper arm. Participants were carefully monitored for ≥30 min after administration for assessment of reactogenicity. Medical interview, phonacoscopy, blood pressure, pulse rate, body temperature, and 12-lead electrocardiogram were performed before and 2 h after administration. Follow-up visits were scheduled from day 4 up to week 52 to discuss any changes in concomitant medications, to collect vital signs, review adverse events, and obtain blood samples for immunogenicity analyses.

Outcomes

Trial outcomes were prespecified in the study protocol and did not change following trial commencement. The primary safety endpoints were the occurrence of solicited local and systemic adverse events that occurred up to 6 days (Day 7) after study drug administration, and any unsolicited adverse events that occurred up to 4 weeks after study drug administration. Information on all adverse events was collected until week 4. Information on serious adverse events, adverse events of special interest, medically-noteworthy or treatment-emergent adverse events as determined by the principal investigator or sub-investigators, and adverse events leading to study discontinuation were collected until the end of study (week 52) or study discontinuation.

The primary immunogenicity endpoints were neutralising antibody titers against SARS-CoV-2 variants up to 26 weeks after study drug administration. Pseudovirus neutralising antibody titers were calculated as 50% inhibitory dilution (ID_{50}), and changes before and after administration of VLPCOV-01 were compared with placebo and BNT162b2. Neutralising activity was assessed against the SARS-CoV-2 spike protein for Wuhan (wild-type), Delta (B.1.617.2), and Omicron (BA.2) variants. Reported secondary immunogenicity assessments were serum IgG titers against SARS-CoV-2 RBD, IgG subclass fraction, and angiotensin-converting enzyme 2 (ACE2)-binding inhibitory activity up to 52 weeks after study drug administration. For quantification of IgG titers in serum, samples were analyzed using the SARS-CoV-2 IgG II Quant assay, which detects IgG antibodies to the RBD of the SARS-CoV-2 spike protein, according to the manufacturer's instructions (Abbott Laboratories). Inhibition of RBD binding to ACE2 was evaluated by V-PLEX SARS-CoV-2 Panel 7 (Meso Scale Diagnostics, LLC). Reported exploratory endpoints were intracellular cytokine staining of antigen-specific $CD4^+$ T-cells.

Assessment of T cell responses

For analyzing antigen-specific T cells, flow cytometric analysis was performed. The cell staining protocol has been previously described.[32] Briefly, peripheral blood mononuclear cells (PBMCs) obtained from participants were incubated in 200 μL RPMI medium containing 10% FBS with or without peptides (17-mers overlapping by 10 residues) corresponding to the RBD region or the full SARS-CoV-2 spike region, at a final concentration of 2 μg/mL of each peptide in the presence of anti-CD107a (H4A3). Thereafter, 0.2 μL BD GolgiPlug and 0.14 μL BD GolgiStop (both from BD Biosciences) were added to the cells and the cells were incubated for 5.5 h. The cells were then stained using the LIVE/DEAD Fixable Blue Dead Cell Stain Kit (Thermo Fisher Scientific) and stained with anti-CD3 (SP34-2), anti-CD4 (S3.5), anti-CD8 (RPA-T8), anti-CD27 (1A4CD27), and anti-CD45RO (UCHL1) antibodies. After fixation and permeabilization using the Cytofix/Cytoperm kit (BD Biosciences), the cells were stained with anti-IFN-g (4S.B3), anti-TNF (MAb11), anti-CD154 (TRAP1), anti-IL-13 (JES10-5A2), anti-IL-21 (3A3-N21), anti-IL-4 (8D4-8), anti-IL-17A (BL168), and anti-IL-2 (MQ1-17H12) antibodies. After washing, the cells were fixed with 1% paraformaldehyde and analyzed using a FACSymphony A5 instrument equipped with five lasers (BD Biosciences). Data were analyzed using the FlowJo software version 10.7.1 (BD Biosciences). After gating live single T-cells, based on forward scatter area and height (FSC-A and -H), side scatter area (SSC-A), live/dead cell exclusion, and CD3 staining, we separated the peripheral blood mononuclear cells (PBMCs) into $CD4^+$ and $CD8^+$ T-cells. Subsequently, $CD4^+$ and $CD8^+$ T-cells were further divided into memory phenotypes based on the expression of CD27 and CD45RO. For spike-specific $CD4^+$ T-cells, memory cells were gated based on the expression of CD154. We defined $CD154^+CD4^+$ T-cells expressing IFN-g, TNF, or IL-2 as Th1 cells, expressing IL4 or IL-13 as Th2 cells, expressing IL-17 as Th17 cells, and expressing IL-21 as $IL\text{-}21^+$ cells. The background of frequencies of cytokine production (measured in DMSO control) were subtracted.

Pseudovirus production

The DNA sequences of SARS-CoV-2 spike gene (Wuhan spike: NC_045512.2, Delta spike: QWA53965.1, Omicron BA.2 spike: UFO69279.1) were codon-optimized for human cells and inserted into eukaryotic expression vactor pCAGG to generate the envelope plasmids. The envelop plasmid was transfected into HEK293T cells by TransIT-LT1 (Mirus Bio) and incubated for 24 h at 37°C. The

cells were infected with the VSVΔG-Luc/G, in which the G envelope was replaced with the reporter luciferase gene, and which was pseudo-typed with the VSV-G glycoprotein.[31,33] The virus was absorbed, washed, and incubated for 24 h at 37°C. The culture supernatant was collected and stored at −80°C after removal of cell debris by centrifugation.

Pseudovirus neutralization assay

The Vero cells (1.5×10^4 cells per well) were seeded on 96-well plate and incubated overnight at 37°C. The serum samples were inactivated at 56°C for 30 min and diluted from 10 to 40,960 dilution with DMEM medium. 60 μL of diluted serum sample was mixed with the equal volume of pseudo-typed virus (equivalent to 2.5×10^6 RLU/mL) for 1h at 37°C. Then, 100 μL of mixture (serum/pseudo virus) was added to the Vero cells and incubated for 24 h at 37°C. The cells were lysed and activated with the Luciferase Assay system (Promega). Luciferase activity of the cells were measured by Synergy LC (Bio Tek). The neutralization activity was analyzed by using GraphPad Prism 8. RLU reduction (percentage) was calculated as: 1-(RLU of samples – RLU of pseudo-typed virus only wells)/(RLU from medium only wells) x 100 (%). The neutralization titer was calculated as 50% inhibitory dilution (ID_{50}).

ACE2 binding inhibition

Inhibition of ACE2 binding to SARS-CoV-2 S1 RBD (wild-type, Alpha and Gamma), and SARS-CoV-2 Spike (wild-type, Alpha, Beta and Gamma) were measured using the V-PLEX COVID-19 Coronavirus Panel 7 (ACE2) multiplexed immunoassay kit (Meso Scale Diagnostics, Rockville, MD USA. Cat.#K15440U-2). The assays were performed according to manufacturer's instructions. Briefly, antigen-coated 96-well plates were blocked with MSD Blocker A for 30 min. Following 3 washes with MSD wash buffer, samples (diluted 1:10 or 1:80 in diluent buffer) or standard solutions were added to the wells. After 2-h incubation, ACE2 Detection Solution (SULFO-TAG Human ACE2 Protein, 1/200 dilution, Cat.#D21ADG-3) was added. Following 3 washes, MSD GOLD Read Buffer B was added to the wells, and plates were read using a MESO QuickPlex SQ 120MM Reader. The standard curve was established by fitting the signals from the standard using a 4-parameter logistic model. Concentrations (Units/mL) of samples were determined from the electrochemiluminescence signals and multiplied by the dilution factor.

Quantitative assessment of anti-RBD IgG subclasses

The plasma levels of each subclass of IgG-targeting SARS-CoV-2 RBD antibodies were determined by ELISA. Recombinant RBD protein was obtained from SinoBiological (Beijing, China). To calculate RBD-specific antibody titers, 96-well plates were coated with SARS-CoV-2 RBD protein and incubated overnight at 4°C. The plates were then washed and incubated for 1 h with blocking buffer, then washed again, and incubated with diluted plasma samples for 2 h at 25°C. For calculation of the concentration of each IgG subclass in plasma, a dilution series of standard antibodies (Anti-SARS-CoV-2 Spike RBD Neutralizing Antibody (AS35), Human IgG1, IgG2, IgG3, or IgG4, (ACROBiosystems, Newark, DE) was also coated on the plate. Next, the plates were washed and incubated with each secondary anti-human IgG; mouse anti-Human IgG1 Fc secondary antibody-HRP (Thermo Fisher Scientific, Waltham, MA), mouse Anti-Human IgG2 Fc-BIOT (SouthernBiotech, Birmingham, AL), mouse Anti-Human IgG3 Hinge-BIOT (SouthernBiotech, Birmingham, AL), or mouse Anti-Human IgG4 Fc-BIOT (SouthernBiotech, Birmingham, AL) for 1 h. For IgG2, IgG3, and IgG4, the plates were then washed and incubated with HRP-conjugated streptavidin (Thermo Fisher Scientific, Waltham, MA) for 1 h at room temperature. The plates were then washed and incubated with TMB peroxidase substrate (KPL, Gaithersburg, MD) for color development. After 10 min, 2 mol/L H_2SO_4 was added to each well to stop the reaction. Antibody expression was measured by determining optical density at 450 nm using an Epoch 2 Microplate Spectrophotometer (Agilent, Santa Clara, CA). The antibody concentration in plasma was measured using standard antibodies.

QUANTIFICATION AND STATISTICAL ANALYSIS

This report presents interim analyses following data cutoff at day 29, when the study was unblinded. No participants were excluded from the full analysis set (FAS). The safety evaluable set (SES) included all participants who received the study drug after randomisation. Among the SES, safety assessments for solicited adverse events were performed for the participant population where diary solicited adverse event data were available. Safety analyses were presented as numbers and percentages of participants who experienced solicited local and systemic adverse events up to 6 days after study drug administration (day 1 to day 7), and adverse events up to 4 weeks after study drug administration. Two-sided 95% confidence intervals (CI) were calculated using the Clopper-Pearson method. One-sided 95% CIs were used for the upper limit when the proportion was 0, or the lower limit when the proportion was 1. For immunogenicity results, mean titers were calculated by log transformation of source data, and two-sided 95% CIs were based on the t-distribution of the geometric mean. Comparisons between groups were determined by estimated geometric mean titer ratios and two-sided 95% CIs. All statistical analyses were performed using the SAS for Windows version 9.4 (SAS Institute Inc., NC, USA). Results of immunogenicity testing beyond the primary time point (day 29; week 4) excluded results for participants who were infected with SARS-CoV-2 or who received other authorised COVID-19 vaccines during the observation period (Table S2).

ADDITIONAL RESOURCES

The trial is registered at the Japan Registry of Clinical Trials under the registration ID jRCT2051210164.

Cell Reports Medicine, Volume *4*

Supplemental information

Safety and immunogenicity of SARS-CoV-2 self-amplifying RNA vaccine expressing an anchored RBD: A randomized, observer-blind phase 1 study

Wataru Akahata, Takashi Sekida, Takuto Nogimori, Hirotaka Ode, Tomokazu Tamura, Kaoru Kono, Yoko Kazami, Ayaka Washizaki, Yuji Masuta, Rigel Suzuki, Kenta Matsuda, Mai Komori, Amber L. Morey, Keiko Ishimoto, Misako Nakata, Tomoko Hasunuma, Takasuke Fukuhara, Yasumasa Iwatani, Takuya Yamamoto, Jonathan F. Smith, and Nobuaki Sato

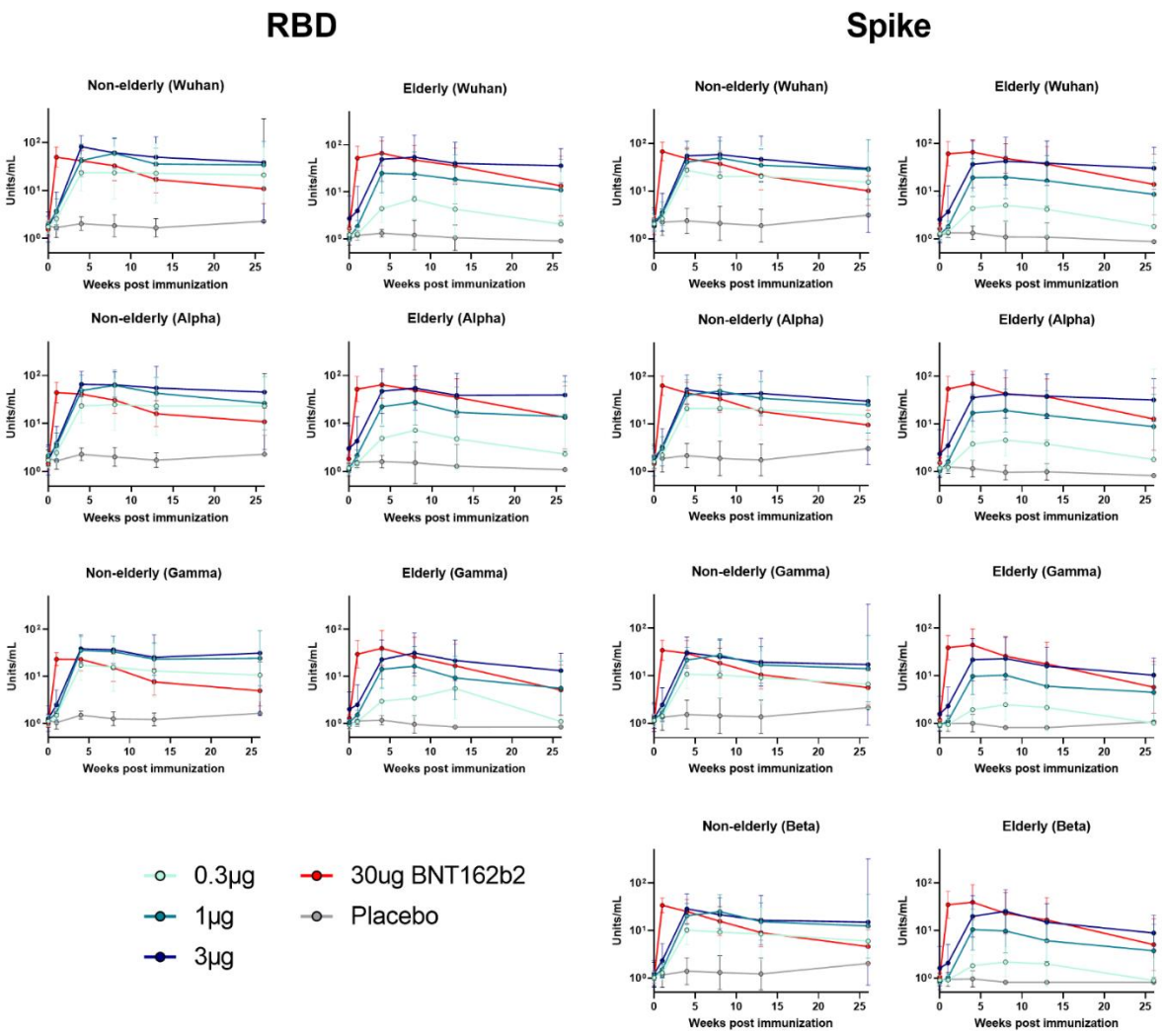

Figure S1: ACE2 Binding Inhibition, related to Figure 3.
The ACE2 and SARS-CoV-2 RBD (Wuhan, Alpha and Gamma) binding inhibition titers (Left panel, RBD) and the ACE2 and SARS-CoV-2 Spike (Wuhan, Alpha, Beta and Gamma) binding inhibition titers (Right panel, Spike) were measured (n = 10 per dose group, and n = 6 for the placebo with 1 technical repeat).

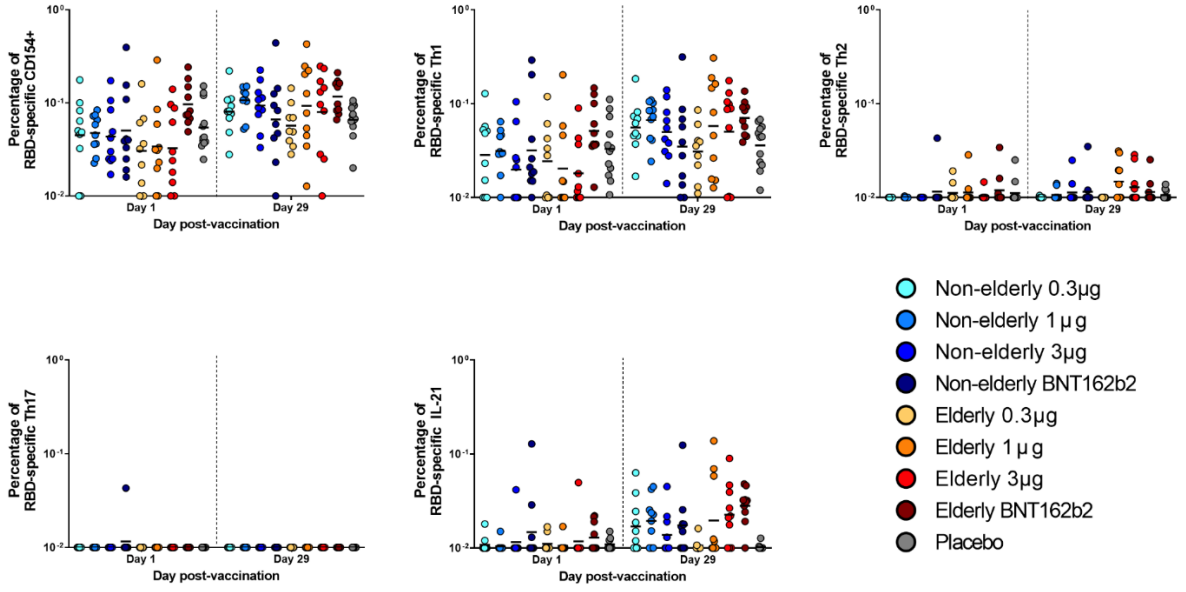

Fig. S2: Absolute RBD-specific CD4$^+$ T-cell Responses, related to Figure 4.
Flow cytometric analysis was performed to measure RBD- or Spike-specific T cells responses. Responses to VLPCOV-01, BNT162b2, or placebo are shown as absolute numbers of responses on baseline (day 1) and week 4 (day 29) for each cohort (top left panel) (n = 10 per dose group, and n = 6 for the placebo group). The top middle panel shows the absolute numbers of response in CD4+ Th1 cells, characterized by the expression of interleukin-2, tumor necrosis factor α, and/or interferon-γ. The top right panel shows the absolute numbers of response in CD4+ Th2 cells, which was measured by expression of interleukin-4 and/or interleukin-13. The bottom left shows the response in CD4$^+$ Th17 cells, characterized by the expression of interleukin-17. The bottom right panel shows the CD4$^+$ IL-21$^+$ cells, which was measured by expression of IL-21. The horizontal bars indicate geometric mean values.

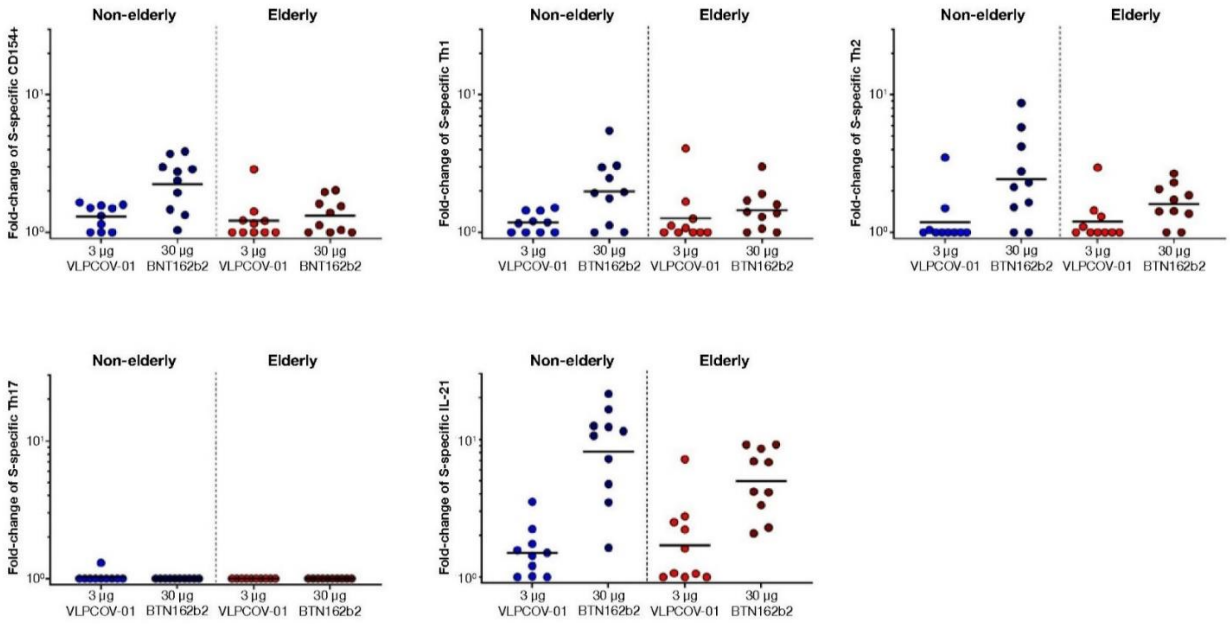

Figure S3: Spike-specific CD4$^+$ T-cell Responses, related to Figure 4.
Flow cytometric analysis was performed to analyse Spike-specific T cell responses. Responses to VLPCOV-01, BNT162b2, or placebo are shown as fold-change from baseline (day 1) to week 4 (day 29) for each cohort (n = 10 per dose group, and n = 6 for the placebo group). Top left panel shows the activated CD4$^+$ T-cells, which was characterised by the expression of CD154$^+$. Top middle panel shows the response in CD4$^+$ Th1 cells, which was characterised by the expression of interleukin-2, tumour necrosis factor α, and/or interferon-γ. Top right panel shows the response in CD4$^+$ Th2 cells, which was measured by expression of interleukin-4 and/or interleukin-13. The bottom left shows the response in CD4$^+$ Th17 cells, characterized by the expression of interleukin-17. The bottom right panel shows the CD4$^+$ IL-21$^+$ cells, which was measured by expression of IL-21. The horizontal bars indicate geometric mean values.

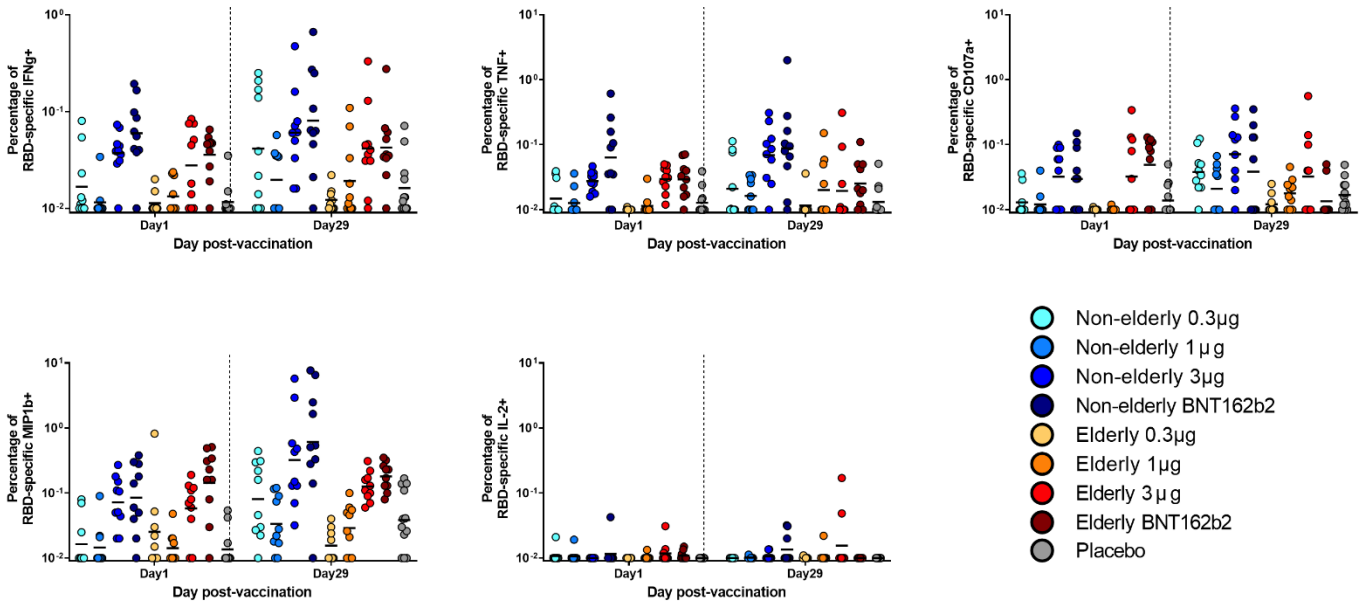

Figure S4: Absolute RBD-specific CD8⁺ T-cell Reponses, related to Figure 4.

Flow cytometric analysis was performed to analyze RBD-specific CD8 T cells responses. Responses to VLPCOV-01, BNT162b2, or placebo are shown as absolute numbers of responses on baseline (day 1) and week 4 (day 29) for each cohort (n = 10 per dose group, and n = 6 for the placebo group). CD8+ cells expressing interferon-γ (top left), tumor necrosis factor α (top middle), CD107a (top right), Macrophage inflammatory protein 1b (bottom left), or interleukin-2 (bottom right) are shown. The horizontal bars indicate geometric mean values.

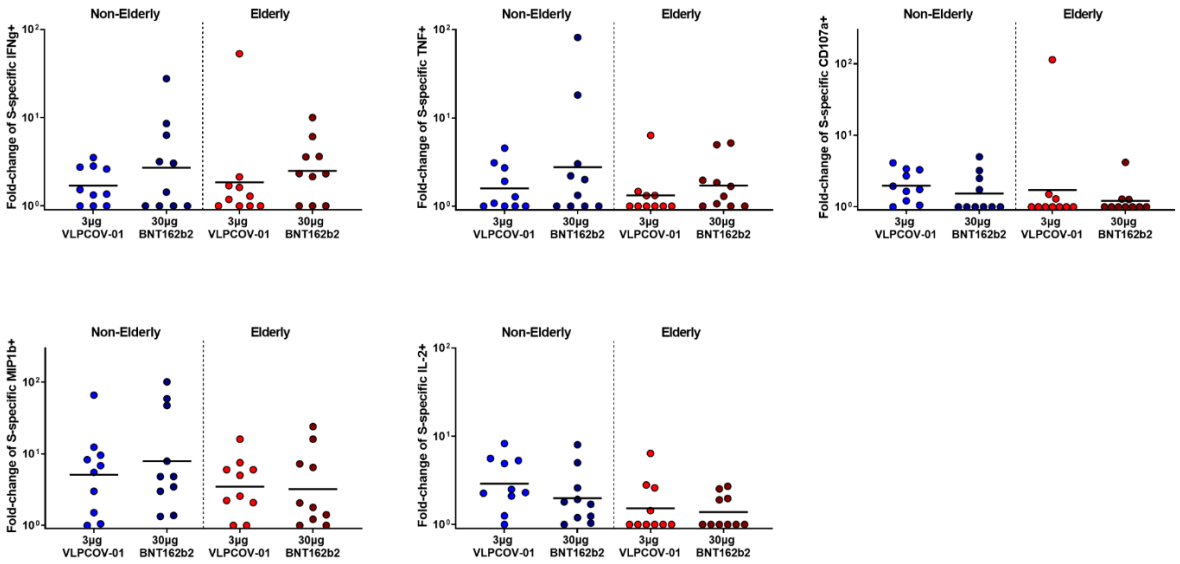

Figure S5: Spike-specific CD8$^+$ T-cell Responses, related to Figure 4.
Flow cytometric analysis was performed to analyse Spike-specific T cells. Responses to VLPCOV-01, BNT162b2, or placebo are shown as fold-change from baseline (day 1) to week 4 (day 29) for each participant (n = 10 per dose group, and n = 6 for the placebo group). Panels show the CD8$^+$ cells expressing interferon-γ (top left), tumor necrosis factor α (top middle), CD107a (top right), Macrophage inflammatory protein 1b (bottom right), or interleukin-2 (bottom right). The horizontal bars indicate geometric mean values.

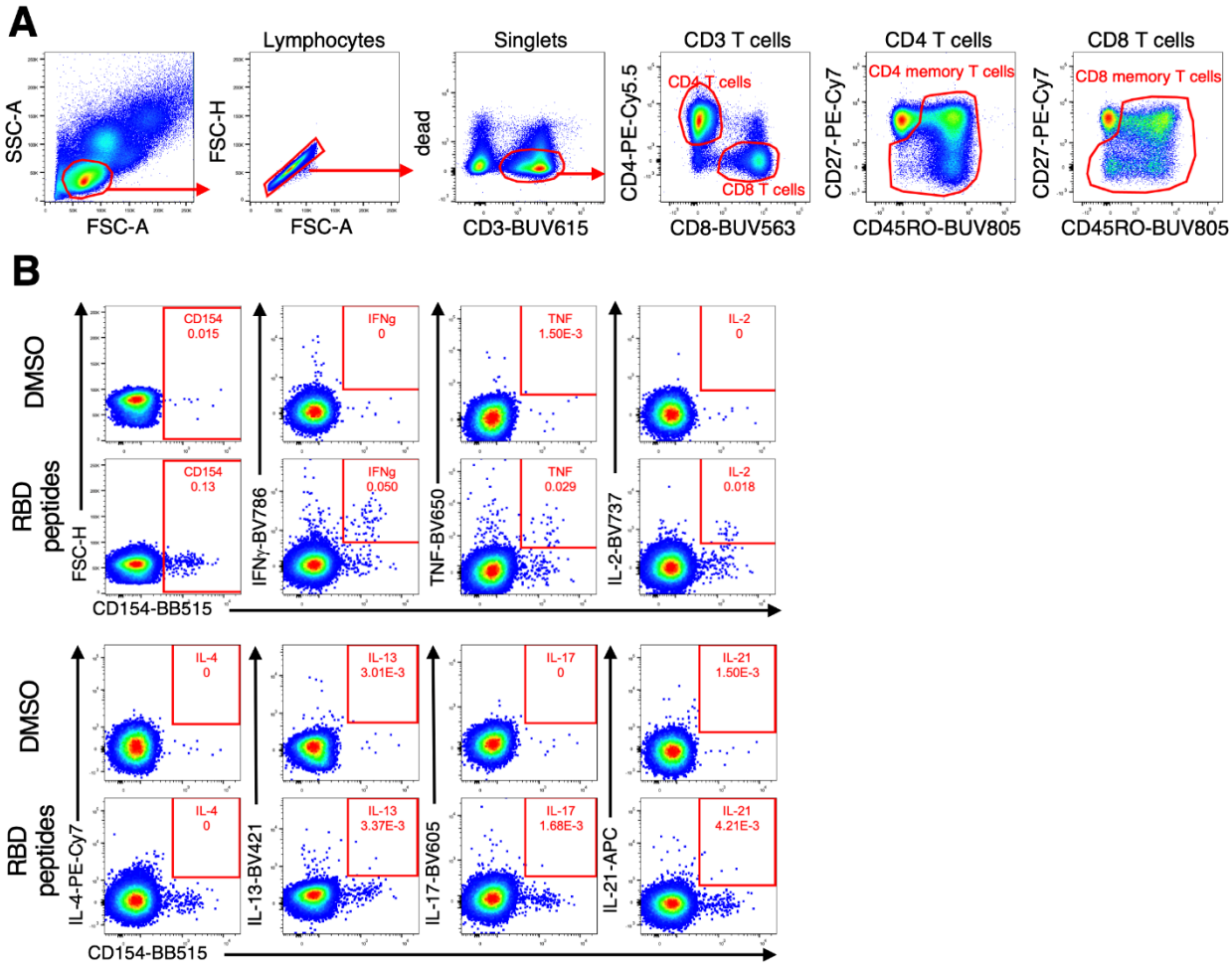

Figure S6. Representative gating strategy for T cell analysis, related to Figure 4.

A) The top 6 panels show the strategy for separation of the peripheral blood mononuclear cells (PBMCs) into $CD4^+$ and $CD8^+$ T-cells. **B)** Subsequently, $CD4^+$ and $CD8^+$ T-cells were further divided into memory phenotypes based on the expression of CD27 and CD45RO. The following panels show the gating strategy for RBD-specific cells expressing various phenotypic markers (CD154, IFN-g, TNF, IL-2, IL4, IL-13, IL-17 and IL-21). The background of frequencies of cytokine production (measured in DMSO control) were subtracted.

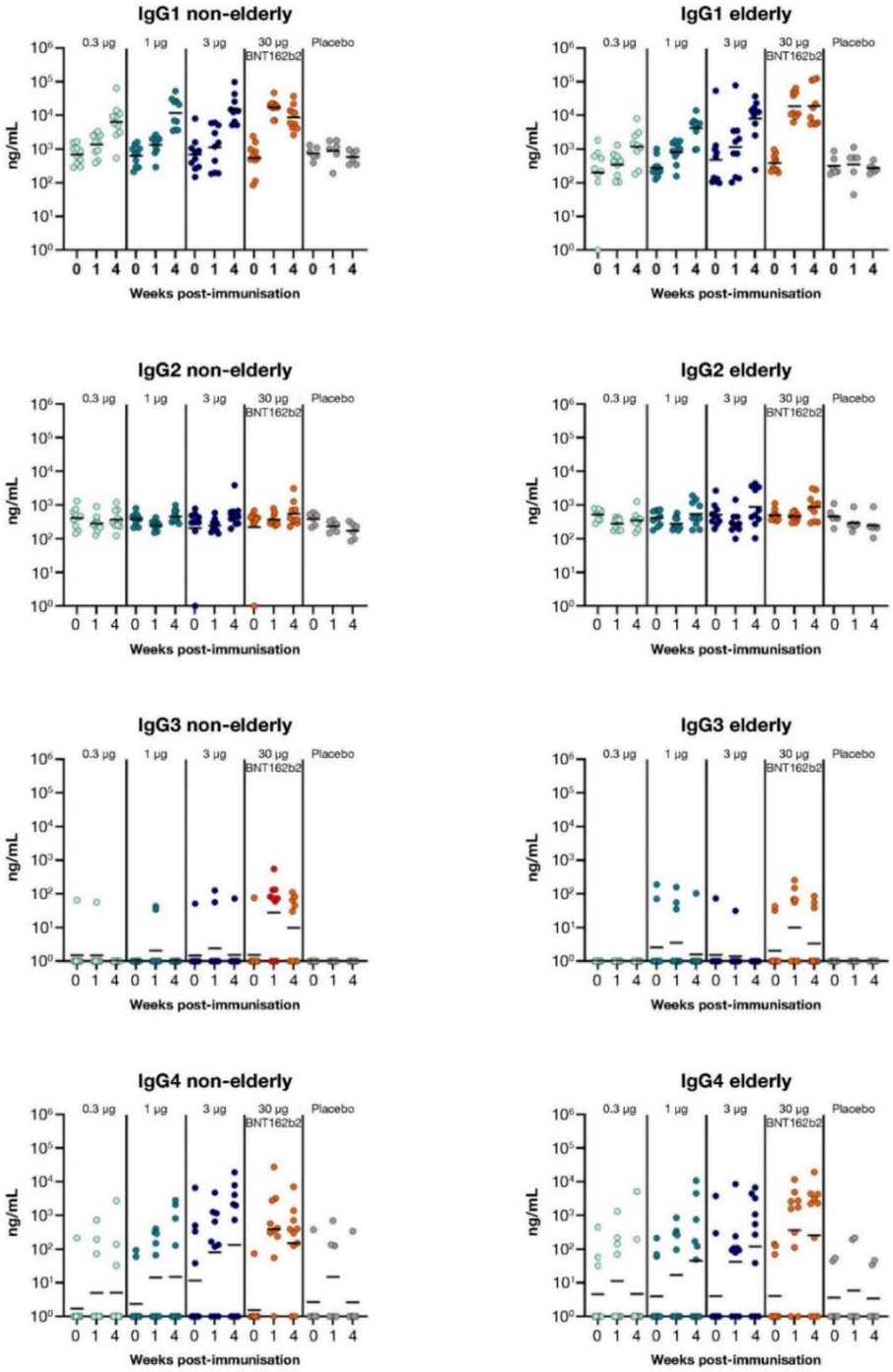

Figure S7. IgG Subclass Analysis, related to Figure 3.

Serum concentration of IgG subclass in study participants was analyzed. Serum concentration of IgG1, IgG2, IgG3, and IgG4 in non-elderly (right panel) and elderly (right panel) groups are measured at 0, 1, and 4 weeks post immunization (n = 10 per dose group, and n = 6 for the placebo group). The concentration of each anti-RBD IgG subclass in plasma was calculated based on a dilution series of standard antibodies. The horizontal bars indicate geometric mean values.